UNIVERSITY OF ZULULAND

Extraction of Cellulose from SCB and its Applications in CNC/Metal Nanocomposites

By

Zimele N.T. Mzimela

201100358

B. Sc. (Hons) (University of Zululand)

THESIS

Submitted in Fulfillment of the Requirements for the Degree

MASTER OF SCIENCE IN CHEMISTRY

Faculty of Science and Agriculture

University of Zululand

Supervisor: Prof. N. Revaprasadu **Co-Supervisor: Prof. T.E. Motaung**

Department of Chemistry, University of Zululand,

Private Bag X1001, KwaDlangezwa, 3886,

South Africa.

February 2018.

DECLARATION

I hereby declare that the work described in this thesis entitled “Extraction of Cellulose from SCB and its Applications in CNC/Metal Nanocomposites” is my own work and has not been submitted in any form for another degree or qualification of the University of Zululand or any other University or Institution of tertiary education. Information derived from the published or unpublished work of others has been acknowledged in the text and a list of references is given.

Name: Zimele N.T. Mzimela

Signature..... Date.....

CERTIFICATION BY SUPERVISORS

This is to certify that this work was carried out by Mr. Zimele N.T. Mzimela in the Department of Chemistry, University of Zululand and is approved for submission in fulfillment of the requirements for the degree of Master of Science in Chemistry.

.....

Supervisor

N. Revaprasadu (PhD)

Professor of Inorganic Chemistry

Department of Chemistry, University of Zululand,

KwaDlangezwa, South Africa.

.....

Co-Supervisor

T.E. Motaung (PhD)

Associate Professor of Organic Chemistry

Department of Chemistry, University of Zululand,

KwaDlangezwa, South Africa.

DEDICATION

This work is dedicated to my mum, dad, sister, two brothers and my late aunt, Nonhlanhla Mzimela. May her soul rest in eternal peace.

ACKNOWLEDGEMENTS

I would like to convey my cordial gratitude to my supervisors, Prof. N. Revaprasadu and Prof. T.E. Motaung for their motivation, patience and colossal knowledge. Their guidance helped me throughout this research and writing of this thesis. I would also like to gratefully acknowledge the financial support from NRF/DST through SARChi granted to Prof. N. Revaprasadu, which enabled me to pursue this study without any hindrances.

I am equally thankful to Dr. Z.L. Linganiso and Dr. M. Mochane for the remarkable roles they played in ensuring the success of this work.

I would also like to thank the entire staff of the Chemistry Department of University of Zululand and also my colleagues and lab mates; Siphamandla Masikane, Sandile Khoza, Fr. Charles Gervas, Sixberth Mlowe, Malik Dishad, Zikhona Tshemese, Zamani Ncanana, Zama Dube and all visiting and former students for their support and assistance during this journey.

I am also very thankful to my colleagues at Foskor, Richards Bay, for their constant support and motivation.

Last but not least, I would like to thank my family, most importantly my parents for their constant spiritual and emotional support throughout this journey.

Table of Contents

ABSTRACT

The past few years have seen an increased interest in enforcing the principles of green chemistry in the scientific community. The aim of these principles is to reduce chemical related impacts on human health and virtually eliminate contamination of the environment through dedicated and sustainable prevention programs.

In the present study, of the many (12) green chemistry principles, we have put into implementation waste prevention, the use of safer solvents and/ or auxiliaries in syntheses, and the use of less hazardous chemicals in syntheses by undertaking a project that makes use of sugarcane bagasse, which is an agricultural waste material obtained when sugarcane is crushed to extract its juices during the production of sugar. From bagasse, cellulose was extracted through five different methods. Through acid hydrolysis, cellulose nanocrystals were synthesised from the extracted cellulose and in turn used as a template, reducing- and stabilizing agent in the synthesis of cellulose nanocrystal/metal (silver and gold) nanocomposites.

The fifth cellulose-extraction method yielded the most thermally stable and pure cellulose. This was shown by TGA and XRD analyses. As a result, the cellulose extracted through the fifth method was used to synthesize cellulose nanocrystals, which were then successfully used as a stabilizing and reducing agent in the formation of CNC/metal nanocomposites, as evident from FTIR, TGA, XRD, UV and TEM analyses.

List of Figures

List of Tables

List of abbreviations

SCB	Sugarcane bagasse
CNCs	Cellulose nanocrystals
CNC/Ag	Cellulose/silver nanocomposite
CNC/Au	Cellulose/gold nanocomposite
CI	Crystallinity index
AgNP	Silver nanoparticles
AuNP	Gold nanoparticles

Techniques and methods

TEM	Transmission electron microscopy
SEM	Scanning electron microscopy
XRD	X-ray diffraction
UV/Vis	Ultraviolet/visible spectroscopy
OM	Optical microscopy
FTIR	Fourier transform infrared spectroscopy
TGA	Thermal gravimetric analysis
DTG	Derivative thermo-gravimetric analysis

Symbols and constants

θ	Theta
λ	Wavelength
kV	Kilovolt
mA	Milliampere

ºC	Degree Celsius
Å	Angstroms

CHAPTER ONE:

GENERAL INTRODUCTION

1.1. Introduction

The syntheses and application of nanoscale materials and structures, especially those ranging from 1 to 100 nm, is a fast growing area of nanotechnology. This is largely due to the fact that nanomaterials have the potential to render solutions to a vast number of environmental and technological concerns in areas such as medicine,[1] catalysis,[2] solar energy conversion[3] and water treatment,[4] to mention but a few. The large applicability of these materials may be attributed to their exhibition of exceptional thermal,[5] optical,[6] physical[7] and chemical properties[8] that are due to their very small sizes, which imply the feasibility of combining a large number of high-energy surface atoms in contrast to the bulk counterparts.

The morphology, size, stability, chemical and physical properties of nanomaterials are highly influenced by the adsorption processes of stabilizing agents with metal nanoparticles, the kinetics of interaction of metal nanoparticles with reducing agents, and most importantly, the synthetic methods and conditions.

The synthesis and stabilization of metal nanoparticles is achieved through physical and chemical routes.[9-12] The chemical routes, which are the mostly used, comprise of methods such as solvothermal reduction,[13] electrochemical techniques[14] and chemical reduction.[15] The major limitation with these methods, however, is that they make use of toxic reducing and capping agents,[16, 17] which may cause severe pollution to the environment in the event that large scale nanoparticles are produced. The reducing and capping agents may also compromise the applicability of the nanomaterials, for example, it is not entirely feasible to use harsh reducing agents in the synthesis of nanomaterials that are used in biological systems.[18] In view of this, a move towards greener synthetic methods is seen as imminent, if not long overdue in the scientific community.

Green chemistry may be defined as a chemical philosophy, or rather, a set of principles (twelve) that encourage the design of processes and products that reduce or eliminate the use and generation of toxic and hazardous substances.[19] The aim of these principles is to reduce chemical related impacts on human health and essentially eliminate contamination of the environment through dedicated and sustainable prevention programs.[19, 20] The combination of nanotechnology with the practices and principles of green chemistry is seen by many as a key factor in the building of an environmentally healthy and sustainable society. This has brought about the coinage of the term of “green nanotechnology”, which basically implies the

incorporation of green chemistry principles into nanotechnology. Green nanotechnology has not only the potential to enhance environmental quality, but also to reduce pollution and conserve natural and non-renewable resources.

The increased attention into the implementation and preservation of the principles of green chemistry, and subsequently green nanotechnology has elevated research into new synthetic routes that can ensure the utilization of environmentally friendly solvents and reaction conditions, and also the use of less hazardous reducing and stabilizing agents in the synthesis of nanoparticles that have the ability to degrade with ease after use.

1.2. Statement of the research problem

The past few years have seen an increased interest in the synthesis of metal nanoparticles and their nanocomposites since they have the ability to find application in a number of scientific and non-scientific fields, due to their exceptionally small sizes which present a plethora of proficient properties that are different from those of the bulk materials.

However, cellulose- metal nanocomposites, especially those derived from silver and gold have not been subjected to intensive scientific studies. Nanocomposites comprising biopolymers like cellulose have the potential of replacing conventional materials such as synthetic polymers. The properties of nanocomposite materials depend not only on the properties of their individual components but also on morphological and interfacial characteristics arising from the combination of distinct materials. Incorporation of polymers like cellulose with metals to form nanocomposites can allow the exploitation of a variety of formulations depending on envisaged functionalities. Critical studies of these nanocomposites will pave the way to better understanding of the different characteristics and applications of such materials.

1.3. Scope of the work

This work focuses on the extraction of cellulose from sugarcane bagasse and its subsequent application in the synthesis of CNC/Ag and CNC/Au nanocomposites.

1.4. Objectives

The objectives of this work are as follows:

1. To extract and characterize cellulose from sugarcane bagasse.
2. To synthesize and characterize cellulose nanocrystals (CNCs) from cellulose.
3. To synthesize and characterize CNC/Ag nanocomposites.
4. To synthesize and characterize CNC/Au nanocomposites.

1.5. Thesis layout

This thesis is composed of six chapters:

1. Chapter 1: General introduction.
2. Chapter 2: Literature review.
3. Chapter 3: Extraction and characterization of cellulose from sugarcane bagasse.
4. Chapter 4: Synthesis of CNCs from cellulose, their characterization, and their application in the synthesis of CNC/Ag nanocomposites.
5. Chapter 5: Synthesis and characterization of CNC/Au nanocomposites.
6. Chapter 6: Concluding remarks based on the summary of the results obtained in this work.

1.6. References

2. L. Zhang, F.X. Gu, J.M. Chan, A.Z. Wang, R.S. Langer, O.C. Farokhzad, *Clin. Pharma. and Therap.,* 2008, 83(5), 761-769.
3. D. Astruc, F. Lu, J.R. Aranzeaes, *Angew. Chemie*, 2005, 44(48), 7832-7872.
4. P. Wang, A. Abuasci, H.M.P. Wong, M. Svensson, M.R. Andersson, N.C. Greenham, *Nano. lett.¸* 2006, 6(8), 1789-1793.
5. T.A. Dankovich, D.G. Gray, *Environ. Sci. Technol.*, 2011, 45(5), 1992-1998.
6. J.R.J. Delben, O.M. Pimentel, M.B. Coelho, P.D. Candelorio, L.N. Furini, F.A. dos Santos, F.S. de Vincente, A.A.S.T. Deblen, *J. Therm. Anal. and Calirometry,* 2009, 97(1), 433-436.
7. K.L. Kelly, E. Coronado, L.L. Zhao, G.C. Schatz, *J. Phys. Chem. B,* 2003, 107(3),668-677.
8. A. Akbarazadeh, M. Samiei, S. Davaran, *Nano. Res. Lett.,* 2012, 7(1), 144-157.
9. V.S. Zaitsev, D.S. Filimonov, I.A. Presnyakov, R.J. Gambino, B. Chu, *J. Coll. and Interf. Sci.,* 1999, 212(1), 49-57.
10. K. Maaz, A. Mumtaz, S.K. Hasanain, A. Ceylan, *J. Magnetism and Magnetic Mater.*, 2007, 308(2), 289-295.
11. M. Niederberger, N. Pinna, J. Polleux, M. Antonietti, *Angew. Chemie,* 2004, 116, 2320-2323.
12. K. Okuyama, I.W. Leggoro, *Chem. Eng. Sci.*, 2003, 58(3-6), 537-547.
13. T.K. Sun, C.J. Murphy, *J. Am. Chem. Soc.,* 2004, 126(28), 8648-8649.
14. Y. Hou, J. Yu, S. Gao, *J. Mater. Chem.,* 2003, 13, 193-1987.
15. J. Ying, S.S. Chang, C.L. Lee, C.R.C. Wang, *J. Phys. Chem. B,* 1997, 101(34), 6661-6664.
16. Y. Ying, Z.Y. Li, Z. Zhong, B. Gates, Y. Xia, S. Venkateswaran, *J. Mater. Chem.*, 2002, 12, 522-527.
17. K.C. Song, S.M. Lee. T.S. Park, B.S. Lee, *Korean J. Chem. Eng.,* 2009, 26(1), 153-155.
18. M. Liu, M.C. Lin, C.Y. Tsai, C.C. Wang, *Int. J. Heat and Mass Transf.,* 2006, 49(17-18), 3028-3033.
19. J.H. Clark, *Green chem.,* 1999, 1, 1-8.
20. K. Alfonsi, J. Coldberg, P.J. Dunn, T. Fevig, S. Jennings, T.A. Johnson, H.P. Kleine, C. Knight, M.A. Nagy, D.A. Perry, M. Stefaniak, *Green Chem.,* 2008,10, 31-36.

CHAPTER TWO:

LITERATURE REVIEW

2.1. Introduction

Metal nanoparticles are receiving considerable interest and attention in the global scientific community due to their demonstration of considerably enhanced chemical, physical and biological properties in contrast to their bulk counterparts.[1-3] They are, therefore, rapidly being studied and synthesized for their applications in fields such as electronics, catalysis, biotechnology and optics, to mention but a few.[4-6]

The major concern about the synthesis and application of metal nanoparticles, however, is that they are synthesized through methods that make use of highly toxic chemicals as reducing and stabilizing agents. As a result, the past few years have seen intense global efforts aimed at introducing "green" chemistry principles in the synthesis of metal nanoparticles. Green chemistry principles are a set of twelve principles that are aimed towards guiding and minimizing the use of unsafe chemicals and maximizing the efficiency of chemical processes.[7, 8]

In the light of this, and in line with the research work reported in this thesis, this review chapter will focus on natural fibres, with specific interest in sugarcane bagasse (SCB). The chapter will dwell on cellulose and cellulose nanocrystals (CNCs) extracted from SCB (CNCs are seen as potential "green" materials that can be used as both reducing and stabilizing agents in the formation of metal nanoparticles).

The chapter will also focus on the green synthesis of metal nanoparticles, with specific attention given to silver and gold nanoparticles. Silver nanoparticles will be investigated in the specific context of their application as antimicrobial agents in the food packaging industry, and gold nanoparticles will be reviewed in the context of their application in catalysis.

2.2. Natural Fibres

Natural fibres are emerging as light weight, low cost and environmentally superior alternatives to glass fibres in composite materials. These are fibres extracted from sources such as plants and animals. Plant fibres include aloe, stalks, wood, reeds, sisal, hemp, bamboo, coir, flax, cotton, banana, pineapple, kenaf, jute, ramie, oil palm and grasses,[9] while animal fibres include wool and chicken feather.[10] Natural fibres are generally abundant and

inexpensive, despite complications of processing compared to glass fibres. The advantages associated with natural fibres, however, outweigh their drawbacks and this has led to the extensive research of these environmentally-friendly green materials.[11-14]

Plant fibres are basically composed predominantly of lignin, cellulose and hemicelluloses. The hemicelluloses and lignin are embedded in a rigid matrix of cellulose, whilst wax and pectin only occupy about 5 %.[15] Many factors, such as the internal fibre structure, microfibril angle, chemical composition, cell dimensions and defects, which vary in different parts of the plant as well as in different plant species, strongly influence the properties of lignocellulosic natural fibres.[16]

Natural fibres are widely used as reinforcements in the production of eco-friendly composites[17] and non-structural parts of the automotive industries such as car roofs and door panels.[18] For the development of composites with good mechanical properties and environmental performance, increasing the hydrophobicity of the cellulose fibres and increasing the interface between the matrix and fibre becomes a necessity. Low melting point, lack of good interfacial adhesion and poor resistance towards moisture make the use of plant-cellulose fibre-reinforced composites less attractive. However, pre-treatments of plant fibres have shown to result in an increase in surface area, roughness and surface functionality, which in turn compensate for some poor properties of polymer composites.

2.3. Sugarcane Bagasse

Sugarcane bagasse is the fibrous matter that remains after sugarcane has been crushed to extract its juices during the production of sugar. It represents around 30-40 wt. % of the waste materials.[19] It is highly abundant in many countries like Australia, Brazil, South Africa, India, Peru and Australia.[20] In 2008, South Africa alone produced 7.9 million tonnes of bagasse. It is estimated that 5.4×10^8 dry tons of sugarcane are processed each and every year globally. Generally, for every single ton of sugarcane, approximately 280 kg of sugarcane bagasse is generated.[20] This material can be seen as either a waste, affecting the environment, or as a very useful resource when appropriate valorisation techniques are implemented. Sugarcane bagasse is composed of, as the major components, lignin (approximately 23.5 %), hemicelluloses (approximately 28.6 %) and cellulose (around 48.3 %).[21, 22] Due to its relatively low ash content,[23] it has the prospects of finding many applications in contrast to other agro-based residues. Basically, the chemical composition of sugarcane bagasse makes it

superb for applications in the synthesis of composite materials that possess exceptional chemical and physical properties. Bagasse also has the added advantage of low fabricating costs and high quality green end-materials. It has found applications in many sectors; it is converted into energy through combustion especially in sugar industries, it is used in the production of activated carbon, in gasification, in the production of cellulosic ethanol, and in pulping, to mention but a few.

Like other plant cell walls, sugarcane bagasse is composed mainly of two carbohydrate fractions, cellulose and hemicelluloses, that are rooted in a lignin matrix. Lignin is a macromolecule composed of phenol units. It is known to be highly resistant to enzyme attack and bio-degradation, and therefore its content and distribution in sugarcane bagasse and other plant cell walls are recognised as the most important factors determining cell wall resistance to hydrolysis.[24-27] The high content of cellulose in bagasse has made this material of high interest amongst researchers.

2.4. Cellulose and Nanocellulose

Cellulose, which is the most abundant renewable organic material produced and present in the biosphere, has an estimated annual production that is well over 7.5×10^{10} tonnes.[28]This material is widely distributed in plants. It is also found in bacteria, algae, protozoa and invertebrates but to a much lesser extent.

In recent years, deforestation concerns have led to the development of non-wood sources of cellulose. Sugarcane bagasse, which is an agricultural waste, has attracted the attention of researchers as a source of cellulose. This source of cellulose is considered environmental-friendly, as fewer forests have to be cut to produce cellulose.[29]

A major development in the field of cellulose chemistry is the development of nanoparticles of cellulose and cellulose derivatives, which are biocompatible and biodegradable. Their roles in several biomedical applications, biosensors, diagnostic molecular probes, drug delivery vehicles, etc are being vigorously pursued, along with other exciting applications in biocomposites, membranes, electronics and solar cells.[30-33]

Cellulose-based nanomaterials have low density, high aspect ratio, good mechanical properties, low thermal expansion, low toxicity and surfaces having hydroxyl groups (-OH) that can be readily functionalized.[34, 35] There are two general classes of cellulose nano objects

that can be extracted from different sources such as plants, animals or mineral plants. They are cellulose nanocrystals (CNCs) and cellulose nanofibrils (CNFs). Cellulose nanocrystals can be referred to as cellulose nanowhiskers (CNWs) or nanocrystalline cellulose (NCC). Cellulose nanofibrils are sometimes referred to as nanofibrillated cellulose (NFC). CNCs are needle-like cellulose particles having at least one dimension equal to- or less than 100 nm, with a highly crystalline nature.[36]

Nanocellulose has been around since the early 1980's.[37] Its production is achieved by delaminating cellulosic fibres in high pressure homogenisers and also by chemical means, usually acid hydrolysis. Fully delaminated nanocellulose consists of long microfibrils and has the appearance of a highly viscous, shear-thinning transparent gel.[38]

The acid hydrolysis of cellulose fibres is known to yield highly ordered rod-like cellulose nanocrystals (CNCs), which are also referred to as nanocrystalline cellulose.[39] Cellulose nanocrystals are highly crystalline, and they have a width of around 2 to 20 nm, and a length up to several micrometers.[40] They have high mechanical properties along the longitudinal direction with an estimated modulus of elasticity of 138 GPa.[41] The coefficient of thermal expansion of crystalline nanocellulose along the longitudinal direction is less than $1\times10^{-7}L.T^{-1}$, which is as small as that of quartz.[42] These excellent features make cellulose microfibrils and cellulose nanofibers promising materials as reinforcements in nanocomposites.

Cellulose microfibrils comprise of amorphous and crystalline regions that have a distribution that is along their length. In the amorphous regions there is greater susceptibility to chemical or enzymatic attack. Cellulose chains are closely packed in the crystalline regions. Cellulose nanocrystals (CNCs) or Nanocrystalline cellulose (NCC) is pure cellulose in crystalline form with nano-scale dimensions. Its production can be from different sources of biomass, yielding liquid, powder or gel forms by the removal of the amorphous regions. The resulting CNCs are rigid rod-shaped in structure, 1-100 nm in diameter and tens to hundred nanometres in length. CNCs are one of the strongest and stiffest natural materials available, and they have a number of intriguing properties, including high tensile strength, high stiffness, high aspect ratio, large surface area and other remarkable electrical and optical properties. CNCs have hydroxyl groups on their surface, which permits further modification to alter their hydrophilicity, prepare biomaterials for targeted applications or provide a stabilization matrix for anchoring metallic nanoparticles.

CNCs can be chemically modified at the hydroxyl groups of the glucose units on the crystalline backbone structure. Reactions to accomplish such modifications include cationization,[43] sulfonation,[44] grafting [45] and silylation.[46]

2.5. Extraction of Cellulose from Natural Fibres

There are many advantages associated with the use of natural fibres. Amongst all, the extraction of cellulose from them has dominated recent literature. It is clear that there are a lot of methods employed for cellulose extraction. It is also worth noting that each and every method gives a different morphology of cellulose, which in most cases affects the final properties and applicability of the material.

Wood is considered a major source of cellulose.[47] However, due to the increasing demands from the paper, building production and furniture industries, the need for low-cost raw materials such as agricultural residues has extensively increased. These materials are considered effective alternative sources for producing cellulose nanofibrils with acceptable properties. Moreover, industrial bioresources usually yield by-products which have great potential for use as cheap and suitable sources for the isolation of cellulose and nanocellulose. As a result, plants such as flax, hemp, sisal, kenaf and agricultural crops such as rice, sugarcane, pineapple and wheat have been largely used.[48-51] In comparison to wood, these crop residues possess positive characteristics such as low contents of hemicelluloses and lignin.

Herrick *et al*[52] and Turbak *et al*[53] produced, in different studies, cellulosic wood pulp-water suspensions through a mechanical homogenizer, in which a large pressure drop facilitated microfibrillation. In another study, an acid-induced destructuring process was used, during which the heterogeneous acid hydrolysis involved the diffusion of acid molecules into cellulose fibres, followed by cleavage of glycosidic bonds. That was followed by centrifugation, dialysis and ultrasonication.[54] Acids such as sulphuric, hydrochloric, phosphoric, nitric, hydrobormic and a mixture composed of hydrochloric and organic acids have been shown to successfully dissolve amorphous regions of cellulose fibres in order to obtain crystalline cellulosic nanoparticles.[55]

The manufacture of microfibrillated cellulose is generally performed by a mechanical treatment consisting of a refining and a high pressure homogenizing process.[56] Cryocrushing

is an alternative method for producing nanofibres. In this method, fibres are frozen using liquid nitrogen before the application of high shear forces. In mechanical treatment equipment, the cellulose slurry is passed between a static grind stone and a rotating grind stone revolving at around 1500 rpm.[57] This method, however, has the huge disadvantage of high energy consumption, which is connected to the mechanical disintegration of the fibres to form microfibrillated cellulose. The mechanical treatment can be combined with some pre-treatments, such as mercerization, in order to decrease the energy consumption.[58] Fibres can be pre-treated with alkali in order to disrupt the cell wall structure and separate the structural linkages.

2.6. Metal Nanoparticles

Inorganic nano-size metallic particles, such as silver, gold, copper and zinc, are not only highly stable but also possess a high surface to volume ratio with increased surface reactivity.[59] Therefore, they have found wide applications in industries for the past two decades. The use of these nanoparticles is currently gaining interest as they also display defined chemical, mechanical and optical properties. Due to their large surface area to volume ratio, some metal nanoparticles, especially silver nanoparticles, display exceptional antibacterial properties. This, along with the growing microbial resistance against antibiotics and metal ions, and also the development of resistant strains, has attracted engineers and researchers towards these materials.[60] A number of metal nanoparticles such as those of copper, titanium, magnesium, gold, alginate, platinum, cobalt, metal alloys and silver have been successfully used as antimicrobial agents.[61-63]

In order to enable the application of antimicrobial agents in the food industry, the industry has to follow the regulations and guidelines of the country in which they are going to be used, for example, FDA (Food and Drug Administration) and/or EPA (Environmental Protection Agency) in the United States. This means that new antimicrobial packaging materials may be developed using only agents which are approved by the authorization agencies as examples of FDA-approved or notified-to-use within the concentration limits for food safety enhancement or preservation. Various antimicrobial agents, such as chemical antimicrobials, antioxidants, biotechnology products, antimicrobial polymers, natural antimicrobials and gas may be incorporated in the packaging system.[64, 65]

The following section will dwell on the applications of silver nanoparticles as antimicrobial agents in the food packaging industry.

2.6.1. Silver Nanoparticles in the Food Packaging Industry

Silver nanoparticles (AgNPs) have attracted special attention in the food packing sector due to their remarkable and broad spectrum of antimicrobial effect against food-borne pathogens. The incorporation of AgNPs into the food packaging system has the ability to effectively obstruct the growth of pathogenic microorganisms.[59] Silver has a long history of being used as an antimicrobial agent in food and beverage storage applications due to the fact that it shows advantages over other antimicrobials. It possesses strong toxicity against a wide range of food-borne pathogens including bacteria, fungi, and some viruses even at very low concentrations.[66] The use of silver nanoparticles has been induced by the fact that several pathogenic bacteria have developed resistance against various antibiotics. The metallic state of silver is inert but it reacts with the moisture in the skin and the fluid of the wound and is then ionized. The ionized silver is highly reactive, binding to tissue proteins and reinforcing structural alterations in the bacterial cell wall and the nuclear membrane which leads to cell distortion and death. Its antimicrobial property is directly proportional to the amount of silver and the rate of silver released. Given the extensive number of products taking advantage of the benefits of silver, it seems sensible to make evaluations of the potential human and ecosystem hazards associated with silver's increased use in the food packaging industry. The main routes of human exposure would be the respiratory system, gastrointestinal system, and skin, which are interfaces between the internal systems of the human body and the external environment.[67] But conventional wisdom regards silver as invulnerable to humans and other higher order organisms when used responsibly, and silver-based pharmaceuticals have few, if any acute or chronic known side-effects at minimal doses. Also, the toxicity of silver complexes of tryptophan and histidine have been tested on a group of white mongrel mice.[68] Both the complexes of histidine and tryptophan showed low toxicity.

2.6.1.1. Synthesis of AgNPs

AgNPs are generally produced through a chemical reduction process. Silver salt is generally dissolved in water with a reducing compound such as $NaBH_4$, citrate, glucose, hydrazine, and ascorbate.[69-71] Very strong reductants lead to generation of small monodispersed particles whereas weaker reductants tend to generate slower reduction reactions. But, recent research has indicated that nanoparticles obtained with weaker

reductants have a tendency of becoming more polydispersed in size. To overcome this drawback, one needs to generate silver nanoparticles with controlled sizes. In doing this, one would use a two-step method. In this method, nuclei particles are prepared using a strong reducing agent and they are enlarged by a weak reducing agent.[72] Unfortunately, reducing agents for silver nanoparticle synthesis are time and again considered toxic or hazardous. As a result, green synthesis methods have been preferred by many researchers.[71, 73] In green synthesis, polysaccharides and polyphenols are generally used as capping agents during silver nanoparticle synthesis, and they may also contribute to the reduction of silver ions. Silver nanoparticles can also be synthesized by irradiating silver salt solutions containing reducing and capping agents. Laser, microwave, ionization radiation, and radiolysis are sources of irradiation that have been used thus far.[74-76] On the other hand, biological methods involve the production of silver nanoparticles utilizing extracts from bio-organisms as reductants, capping agents or both.[77] Proteins, amino acids, polysaccharides, and vitamins are the mostly explored extracts.[75] Other explored plant extracts include leaf extracts from magnolia, persimmon, geranium, and pine leaf,[78-80] to name a few. Silver nanoparticles can also be synthesized by several microorganisms such as the bacterial strains *Bacillus licheniformis, K. pneumonia*, and fungi strains such as *Verticillium* and *Fusarium oxysporum, Aspergillus flavus*.[81] Stoeva and co-workers[82] invented another method of producing AgNPs. In this method, silver nanoparticles were synthesized by the solvated metal atom dispersion (SMAD) method.

2.6.1.2. How Silver Attacks Microorganisms

AgNPs possess a higher antimicrobial effect than ionic silver because they can be interpolated within a cell membrane due to their small sizes and kill bacteria by direct lesion and/or by releasing silver ions locally from the nanoparticles causing damage to bacterial enzymes.[83-85] Furthermore, the antimicrobial activity of AgNPs can be related to the induction of oxidative stress, which may cause damage in the respiratory chain and cell division machinery.[86] But the mechanism of how silver attacks microorganisms remains unresolved. As a result, comprehensive research remains active in this field. Different mechanisms have been proposed to explain the antimicrobial activity of silver nanoparticles. Current findings propose that silver kills by (a) interference with vital cellular processes by binding to sulfhydryl or disulfide functional groups on the surfaces of membrane proteins and other enzymes; (b) disruption of DNA replication; and (c) oxidative stress through the

catalysis of reactive oxygen species (ROS) formation. Hypothesized interactions between AgNPs and bacteria cells are abstractly exemplified in Figure 2.1.

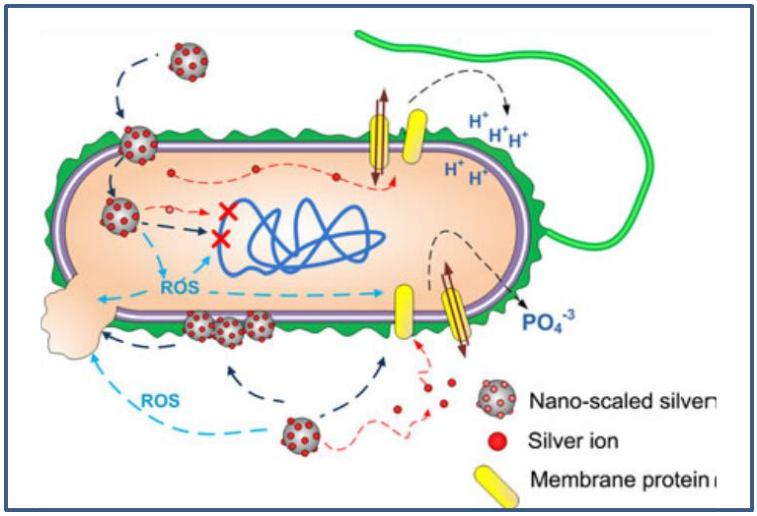

Figure 2.1: A summary of AgNPs interactions with bacterial cells. AgNPs may (1) emancipate silver ions and generate ROS; (2) interact with membrane proteins, thereby affecting their anticipated functionality; (3) accumulate in the cell membrane, thereby affecting the permeability of the membrane; and (4) invade the cell where it can generate ROS, release silver ions, and cause alterations to the DNA.[87, 88]

There has been a lot of controversy around which of these mechanisms is the most vital. Discrepancies were noted on research findings by Dibrov and co-workers [89] and Yamanaka *et al*.[90] Dibrov *et al*. reported that silver binding specifically to membrane proteins disrupts ion and proton transport across the membrane, whereas on the other hand Yamanaka *et al*. showed evidence that Ag ions permeate to the cellular interior, where they interfere with ribosomal activity and derange the production of several key enzymes responsible for the production of energy. Feng and co-workers[91] reported the disruption of cell wall from silver binding to membrane proteins and DNA condensation in *Escherichia coli* and *Staphylococcus aureus*. In this case, DNA condensation in the presence of Ag ions was reported to be a defence mechanism. However, there have been a number of controversies around these mechanisms as reported by Batarseh *et al*.[92] Notwithstanding the discrepancies, all the mechanisms seem to play a crucial role to the antimicrobial activity of silver, which induces the global use of silver nanocomposites to preserve food for human consumption.

2.6.1.3. Silver Nanoparticles and Nanocomposites as Antimicrobial Food Packaging Materials

For the full exploitation of the properties of silver nanocomposites, silver nanoparticles should be well dispersed on the surface of the polymer matrix without the formation of large aggregates which eventually reduces the antimicrobial properties of silver. The particles must be kept as small as possible with a narrow size distribution. The incorporation of silver nanoparticles into different matrices has been exhaustively studied in order to expand their effectiveness. Polymers are highly regarded as great matrices for metal nanoparticles because they bring stability to nanoparticles through electrostatic interaction of their functional groups with the nanoparticles. Antimicrobial activity of silver ions can be assigned to their ability to derange both inner and outer cell membranes. They can also inhibit respiratory chain enzymes and reduce the ATP (Adenosine triphosphate) levels.[93, 94] Recent researches on antimicrobial activity of silver nanoparticles are summarised in Table 1.

Table 1: Summary of antimicrobial packaging systems with AgNPs.[95]

Nanoparticles	**Polymer**	**Tested microorganisms**	**Reference**
Ag/Chitosan	PLA[1]	*Staphylococcus aureus* (ATCC 6538) *Escherichia coli* (DSMZ 30083)	Turalija *et al*. (2016)
Ag	Agar banana powder	*Escherichia coli* *Lysteria monocytogenes*	Orsuwan *et al*. (2016)
TiO_2/Ag/Cu	PVC[2]	Mixed microorganism culture media	Krehula *et al*. (2016)
ZnO/Ag/Cu	PLA[1]/PEG[3]	*Lysteria monocytogenes* *Salmonella typhimurium*	Ahmed *et al*. (2016)
Ag	PE[4]	*Escherichia coli*	Eslami *et al*. (2016)
Ag/Cu	Guar Gum	*Lysteria monocytogenes* *Salmonella typhimurium*	Arfat *et al*. (2017a)
Ag/TiO_2	PE	*Aspergillus flavus*	Li *et al*. (2017)
Ag/Cu	Fish skin gelatin	*Lysteria monocytogenes* *Salmonella enterica* sv Typhimurium	Arfat *et al*. (2017b)
Ag	Starch/PVA[5]	*Lysteria inocua;* *Escherichia coli* *Aspergillus niger;* *Penicillium expansum*	Cano *et al*. (2016)
Ag/SiO_2/TiO_2	LDPE[6]	*Escherichia coli*	Becaro *et al*. (2016)
Ag	PHBV3[7]	*Salmonella enterica* *Lysteria monocytogenes*	Castro-Mayorga *et al*. (2017)

[1]Polylactic acid; [2]Polyvinylchloride; [3]Polyethylene glycol; [4]Polyethylene; [5]Polyvinyl alcohol; [6]Low density polyethylene; [7]poly(3-hdroxybutyrate-co-3mol%-3-hydroxyvalerate).

Various matrices have been used as antibacterial silver nanoparticles supports.[96] A subdivision has been made according to the type of matrix used to host AgNPs. These subdivisions differ according to the polymeric matrix used. If non-degradable polymers are not used to host AgNPs, biodegradable ones are used. In both cases, the incorporation of AgNPs into polymeric matrices significantly affects the film permeability to improve product quality. Polyethylene (PE), polyvinyl chloride and Ethylene Vinyl Alcohol (EVOH) are the most frequently used to host AgNPs for food packaging systems. Positive finding on the shelf life of Chinese jujube were observed when a blend of polyethylene with a powder containing AgNPs, TiO_2NPs and kaolin was evaluated and tested.[97] An *et al* [98] conducted a study in which asparagus was coated with chemically reduced silver nanoparticles dispersed in polyvinyl-pyrrolidone. Its shelf life improved significantly by about 10 days at 2 ^{o}C, when the nanoparticles were on average 15-25 nm in size. Low density polyethylene (LDPE) reinforced with 95 % zinc oxide doping 5 % metal-nanosilver (10 nm) were used to extend the shelf-life of orange juice over 28 days, without impairing juice relevant quality attributes, such as colour or ascorbic acid content.[99] The nanocomposites displayed enhanced antimicrobial properties in combination with heat treatment at the pasteurization temperature (55 to 65 ^{o}C). Del Nobile *et al.*[100] proved that silver-containing polyethyleneoxide-like coating on a polyethylene layer displayed strong antimicrobial activity.

Biobased polymers, and those originating from renewable sources, are largely being utilised as carriers of silver nanoparticles. These polymers are sensitive to humidity and are strongly plasticized due to water sorption, which results in the generation of the uncontrolled release of immobilized active substances; but surface oxidation due to contact with oxygen and the ionic exchange are required to achieve the release of metal ions trapped in the nanoparticles. The antimicrobial activity of the AgNPs, therefore, is a result of the high water sorption created by the hydrophilic nature of biobased matrices.

There is currently growing interest in the production of active AgNPs with potent antimicrobial effect using polysaccharides such as starch,[101] chitosan,[102] agar,[103] pullulan, dextran[104], guar gum[105] and alginate.[106] The effect of incorporating silver and chitosan nanoparticles into PLA has been analysed by Turalija *et al.*[107] In their work they also used plasma treatment for surface modification of polymer matrix as activation of polymer surface and antimicrobial components. This system represents synergetic approach where more than two influences are included for the enhancement of material properties to create active

packaging solutions. Silver/magnetite nanocomposites have specific applications in water disinfection [108, 109] and the particles can be removed by a magnet after the treatment process. Prucek *et al.*[110] synthesized two types of magnetic binary nanocomposites; Ag@Fe_3O_4 and g-Fe_2O_3@Ag. They were synthesized and characterized and their antibacterial activities were tested. As a magnetic component, Fe_3O_4 (magnetite) nanoparticles with an average size of about 70 nm and monodispersed g-Fe_2O_3 (maghemite) nanoparticles with an average size of 5 nm were used. Nanocomposites were prepared via *in-situ* chemical reduction of silver ions by maltose in the presence of particular magnetic phase and molecules of polyacrylate serving as a spacer among iron oxide and silver nanoparticles. Both synthesized nanocomposites exhibited very significant antibacterial and antifungal activities against ten tested bacterial strains (minimum inhibition concentrations (MIC) from 15.6 mg/L to 125 mg/L) and four Candida species (MIC from 1.9 mg/L to 31.3 mg/L). In another study, Sureshkumar and co-workers[111] also prepared magnetic antimicrobial nanocomposites from bacterial cellulose (BC), silver and iron nanoparticles. A combination of iron based magnetic nanoparticles with silver nanoparticles in the nanostructure of BC was found to illustrate an interesting approach to develop recoverable and reusable antibacterial agents. This approach was the first step to expand the unique nature of Ag nanoparticles into a wider range of applications. Easy recovery of Ag nanoparticles for their antimicrobial character could be achieved by using magnetic Ag nanocomposites. Bacteria growth inhibition was investigated and the experimental results showed that approximately 4 h delay was observed and that the growth delay time increased with an increasing concentration of Ag nanoparticles (Figure 2.2).

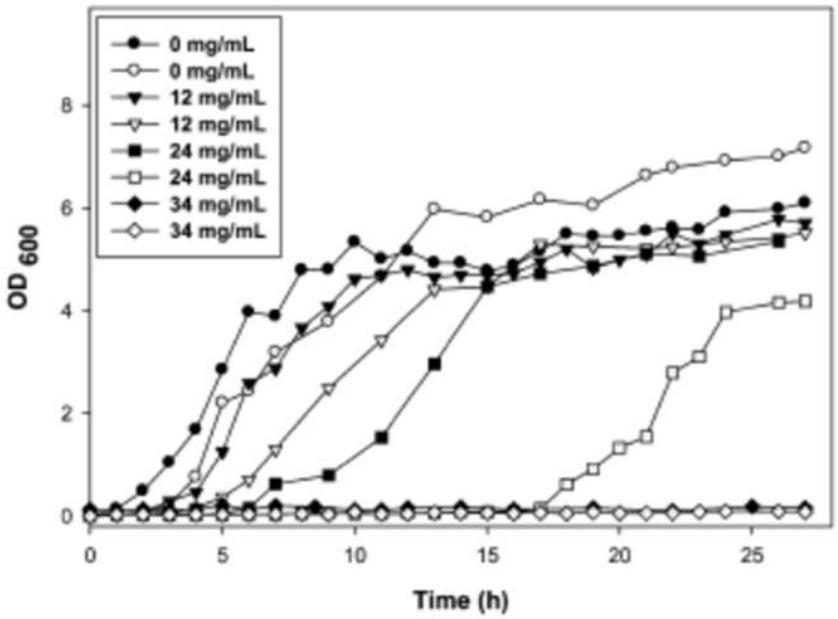

Figure 2.2: Growth curve of E. coli (closed symbol) and B. subtilis (open symbol) in LB liquid medium in the presence of PMBC-Ag for growth inhibition study.[111]

AgNPs/Agar banana powder showed significant antimicrobial activity against *Escherichia coli* and *Lysteria monocytogenes*.[112] The nanocomposites did not only increase the UV light absorption and water barrier properties, but also the antioxidant properties. Silver nanoparticles and nanometal titanium oxide were incorporated into polyvinyl chloride and tested on mixed microorganism culture suspension.[95] A very good antimicrobial activity on tested microorganisms was reported. TiO_2 displayed UV protection while the addition of silver and copper nanoparticles showed improvements in the thermal stability of pristine polymer.[113] Kanmani and Rhim[114] developed gelatin/silver nanoparticle antimicrobial composites. The results of their work showed that gelatin/AgNPs nanocomposite films (30 and 40 mg) exhibited strong antimicrobial activity against Gram-positive and Gram-negative food-borne pathogens. The gelatin/AgNPs composite films with strong antimicrobial activity against both Gram-positive and Gram-negative food-borne pathogenic bacteria can be used as an active food packaging system for extending the shelf-life of foods and maintaining food quality during storage and distribution of the packaged foods. Siqueira *et al.*[115] also investigated the antimicrobial activity of carboxymethyl-cellulose films loaded with silver nanoparticles against gram-positive and gram-negative bacteria for food applications. AgNPs incorporated into polyethylene polymer matrix displayed a strong antimicrobial activity against *E. coli*.[116] AgNPs in low density polyethylene (LDPE) in silver/silica/TiO_2 system also showed antimicrobial activity against *E. coli*.[117] Castro-Mayorga *et al.*[118] reported

prolonged antimicrobial activity against food-borne pathogen (*S. enterica* and *L. monocytogenes),* and drop in oxygen permeability of PHBV3 polymer matrix with silver nanoparticles. A concentration of 60 mg Ag^{+}/kg was necessary to reduce the microbial load by one log unit in absorbent pads in contact with beef meat. Silver loaded cellulose materials were investigated by Pinto *et al.*[119] and Fernandez *et al.*[120] When silver was loaded on different cellulose matrices (fluff pulp cellulose, bacterial cellulose, and EFTe nanostructured cellulose) the resulting nanomaterials displayed different properties, but a reasonably good antimicrobial activity against *Klebsiella pneumoniae, E. coli, S. aureus* and *spore forming B. subtilis* in protein rich cultivation media. Natural chelating agents in food matrices neutralise the antimicrobial influence of silver ions. This reveals a serious drawback strongly limiting the feasibility of this promising technology in food contact applications. In contrast, a higher antimicrobial activity may be expected in the presence of juices with low protein content, such as vegetable or fruit juices.[121] In spite of the high potential of biopolymer/AgNPs composite films for application in active food packaging systems, attention should be paid to the potential toxicity of nanomaterials liberated from the polymer matrix and their migration.

Cellulose based materials are being widely used as they offer advantages including edibility, biocompatibility, barrier properties, attractive appearance, nontoxicity, non-polluting and low cost. de Moura *et al.*[122] investigated the incorporation of AgNPs into hydroxypropyl methylcellulose (HPMC) matrix for applications in food packaging. Mechanical analysis and water vapour barrier properties of HPMC/AgNPs nanocomposites were analysed. The best results were obtained for films containing smaller AgNPs (41 nm). The antibacterial properties of HPMC/AgNPs thin films were evaluated based on the diameter of inhibition zone in a disk diffusion test against *Escherichia coli* (*E. coli*) and *Staphylococcus aureus* (*S. aureus*). The disk diffusion studies revealed a greater bactericidal effectiveness for nanocomposite films containing 41 nm Ag nanoparticles.

Rai *et al.*[123], on the work titled "Silver nanoparticles as a new generation of antimicrobials" reported that silver has been in use since time long-lived in the form of metallic silver, silver nitrate and silver sulfadiazine for the treatment of burns, wounds and several bacterial infections. But due to the emergence of various antibiotics the utilization of these silver compounds has been decreased remarkably. Nanotechnology is obtaining enormous impetus in the current century due to its potential of adjusting metals into their nanosize, which extremely converts the chemical, physical and optical properties of metals.

Metallic silver in the form of silver nanoparticles has made an extraordinary comeback as a potential antimicrobial agent. The use of silver nanoparticles is also significant, as various pathogenic bacteria have enhanced resistance against various antibiotics. Thus, silver nanoparticles have integrated up with diverse medical applications ranging from silver based dressings, silver coated medicinal devices, such as nanogels, nanolotions, etc. The authors noted that among the different antimicrobial agents, silver has been most substantially studied and utilized since ancient times to battle infections and avert spoilage. The antibacterial, antifungal and antiviral properties of silver ions, silver compounds and silver nanoparticles have been extensively studied. Silver is also found to be harmless to humans in minute concentrations. The microorganisms are unlikely to enhance resistance against silver as compared to antibiotics as silver attacks a broad range of targets in the microbes. The silver nanoparticles with their distinct chemical and physical properties are demonstrating as an alternative for the growth of new antibacterial agents. The benefit of utilizing silver nanoparticles for impregnation is that there is continuous release of silver ions and the devices can be coated on both the outer and inner sides thus, developing its antimicrobial efficacy.

Ahmed *et al*.[124] compiled a review in which they reported that metallic nanoparticles are being used in every period of science along with engineering involving medical fields and are yet attracting the scientists to investigate new dimensions for their respective worth which is vaguely accredited to their corresponding small sizes. Findings in research have demonstrated their antimicrobial importance. Among various noble metal nanoparticles, silver nanoparticles have achieved a special focus. They mentioned that silver nanoparticles are regularly synthesized by chemical methods, utilizing chemicals as reducing agents which later on become responsible for various biological risks due to their vague toxicity; endangering the significant concern to enhance environment friendly procedures. Hence, to solve the problem; biological approaches are coming up to fill the void; for instance green syntheses utilizing biological molecules acquired from plant sources are emerging superior over chemical and/or biological methods. These plant-based biological molecules undergo maximum controlled assembly for making them acceptable for metal nanoparticle synthesis. For the synthesis of nanoparticles, employing plants can be advantageous over other biological entities. There is still a demand for commercially viable, economic and environmentally friendly way to find potential of natural lowering constituent to form silver nanoparticles which have not yet been studied. There is a serious variation in chemical

compositions of plants of the same kind when collected from different parts of the world and this may lead to different outcomes in different laboratories. This is the crucial drawback of syntheses of silver nanoparticles using plant extracts as reducing and stabilizing agents and there is a need to resolve this issue. A control of this issue can give a facelift towards the green synthesis of silver nanoparticles.

CaO *et al.*[125] assembled silver nanoparticles by chemical reduction method utilizing chitosan as a stabilizer and ascorbic acid as a reducing agent. In their work, silver/chitosan nanocomposites were analysed using UV spectrophotometer, nano-grain-size analyzer, and transmission electron microscopy. Antibacterial activities of these nanocomposites were carried out for *S. aureus* and *E. coli*. The silver nanoparticles displayed significant inhibition potential towards these bacteria. Detailed studies on the biocompatibility of the silver/chitosan nanocomposites were investigated by 3-(4,5-dimethylthiazol-2-yl)-2,5-diphenyltetrazolium bromide assay and cell adhesion test. The outcomes showed that these silver/chitosan nanocomposites were advantageous for the proliferation and adhesion of L-929 cells, and the biocompatibilities between the nanocomposites and the cells would become better with the culturing days. It is expected that these silver/chitosan nanocomposites could be used as coating material in biomedical engineering and food packing fields wherein antibacterial properties and biocompatibilities are important.

Maneerung *et al.*[126] manufactured bacterial cellulose by *Acetobacter xylinum* (strain TISTR 975). Bacterial cellulose is an interesting material for utilizing as a wound dressing since it presents a moist environment to a wound resulting in a better wound healing. However, bacterial cellulose itself has no antimicrobial activity to avert wound infection. To reach antimicrobial activity, silver nanoparticles were impregnated into bacterial cellulose by immersing bacterial cellulose in silver nitrate solution. Sodium borohydride was then used to reduce the absorbed silver ion (Ag^{+}) inside of bacterial cellulose to the metallic silver nanoparticles (Ag^{0}). Silver nanoparticles showed the characteristic optical absorption band around 420 nm. The red-shift and broadening of the optical absorption band was detected when the mole ratio of $NaBH_4$ to $AgNO_3$ ($NaBH_4$:$AgNO_3$) was reduced. An increase in particle size and particle size distribution of silver nanoparticles was also apparent, as evident from TEM analysis. The development of silver nanoparticles was also indicated by the X-ray diffraction. The freeze-dried silver nanoparticle-impregnated bacterial cellulose presented

strong antimicrobial activity against *E. coli* (Gram-negative) and *S. aureus* (Gram-positive), which are vague bacteria found on polluted wounds.

Impellitteri[127] reported that, because of their antibacterial properties, silver nanoparticles are mostly utilized in consumer products. To evaluate environmental and/or human health risks from these nanoparticles, there is a demand to identify the chemical conversions that silver nanoparticles encounter in different environments. Thus an antimicrobial material containing Ag nanoparticles was inspected by X-ray absorption spectroscopy to identify the speciation of Ag. The material was introduced to a hypochlorite/detergent solution and subjected to agitation. An elemental Ag nano-powder was also introduced to the hypochlorite/detergent solution or to a 1 mol L^{-1} NaCl solution. Outcomes displayed that the material nanoparticles consisted of elemental Ag. After exposure to the hypochlorite/detergent solution, a significant portion of the nanoparticles were changed in situ, to AgCl. Results from exposures to elemental Ag nano-powder suggest that an oxidation step is obligatory for the elemental Ag nanoparticles to convert into AgCl as there was no evidence of AgCl formation in the existence of chloride alone. As a result, if Ag ions leach from consumer products, any chloride present may quickly scavenge the ions. In addition, the efficacy of Ag as an antimicrobial agent in fabrics may be scarce, or even negated after washing in solutions containing oxidizers as AgCl is much less reactive than Ag ion.

Roe *et al.*[128] examined the antimicrobial activity and assessed the risk of systemic toxicity of novel catheters coated with silver nanoparticles. Catheters were coated with silver using $AgNO_3$, a surfactant and *N,N,N ′,N ′*-tetramethylethylenediamine as a reducing agent. Particle size was determined by electron microscopy. Silver release from the catheters was determined *in vitro* and *in vivo* utilizing radioactive silver ($^{110m}Ag^{+}$). The activity on microbial development and biofilm formation was assessed against pathogens most generally included in catheter-related infections, and the risk for systemic toxicity was estimated by measuring silver biodistribution in mice implanted subcutaneously with $^{110m}Ag^{+}$- coated catheters. The results displayed that the coating method yielded a thin (~100 nm) layer of nanoparticles of silver on the surface of the catheters. Variations in $AgNO_3$ concentration translated into proportional converts into silver coating (from 0.1 to 30 μg/cm^2). Sustained release of silver was demonstrated over 10 days. Coated catheters displayed significant *in vitro* antimicrobial activity and averted biofilm formation utilizing *E. coli*, *Enterococcus*, *S. aureus*, *coagulase-negative staphylococci*, *Pseudomonas aeruginosa* and *Candida albicans*.

Approximately 15 % of the coated silver eluted from the catheters in 10 days *in vivo*, with predominant excretion in faeces (8 %), assembled at the implantation site (3 %) and no organ accumulation (≤ 0.1 %). In concluding remarks, the authors noted that a method to coat plastic catheters with bioactive silver nanoparticles was successfully enhanced. These catheters were non-toxic and were capable of targeted and sustained release of silver at the implantation site. Because of their demonstrated antimicrobial properties, they may be useful in decreasing the risk of infectious complications in patients with indwelling catheters.

Jain *et al.*[129] reported that silver is an effectual antimicrobial agent with less toxicity, which is significant especially in the treatment of burn wounds where transient bacteraemia is prevalent and its fast control is crucial. Drugs releasing silver in ionic forms are known to get neutralized in biological fluids and upon long-term use may cause cosmetic abnormality and delayed wound healing. Given its broad spectrum activity, efficacy and lower costs, the search for newer and superior silver-based antimicrobial agents is deemed a necessity. Among the various options available, silver nanoparticles have been the focus of increasing interest and are being heralded as an outstanding candidate for therapeutic purposes. The researchers were able to grow an antimicrobial gel formulation containing silver nanoparticles (AgNPs) in the size range of 7−20 nm synthesized by a proprietary biostabilization procedure. The typical minimum inhibitory concentration (MIC) and minimum bactericidal concentration (MBC) against quality reference cultures as well as multidrug-resistant organisms were reported to be 0.78−6.25 μg/mL and 12.5 μg/mL, respectively. Gram-negative bacteria were killed more effectively (3 $\log_{10}$ decrease in 5−9 h) than Gram-positive bacteria (3 $\log_{10}$ decrease in 12 h). AgNPs also presented good antifungal activity (50% inhibition at 75 μg/mL with antifungal index 55.5 % against *Aspergillus niger* and MIC of 25 μg/mL against *Candida albicans*). When the interaction of AgNPs with generally utilized antibiotics was investigated, the observed effects were synergistic (ceftazidime), additive (streptomycin, kanamycin, ampiclox, polymyxin B) and antagonistic (chloramphenicol). Interestingly, AgNPs presented good anti-inflammatory properties as indicated by concentration-dependent inhibition of marker enzymes (matrix metalloproteinase 2 and 9). The post agent effect (a parameter measuring the length of time for which bacterial development remains subdued following brief exposure to the antimicrobial agent) varied with the kind of organism (e.g., 10.5 h for *P. aeruginosa*, 1.3 h for *Staphylococcus sp*. and 1.6 h for *C. albicans*) indicating that dose regimen of the AgNP formulation should ensure sustained release of the drug. To meet this requirement, a gel

formulation containing AgNPs was prepared. The antibacterial spectrum of the gel was found to be comparable to that of a commercial formulation of silver sulfadiazine, albeit at a 30-fold less silver concentration. As part of toxicity studies, localization of AgNPs in Hep G2 cell line, cell viability, biochemical effects and apoptotic/necrotic capacity were evaluated. It was found that AgNPs get localized in the mitochondria and have an IC_{50} value of 251 μg/mL. Even though they obtain an oxidative stress, cellular antioxidant systems (reduced glutathione content, superoxide dismutase, catalase) get triggered and prevent oxidative damage. Furthermore, AgNPs persuade apoptosis at concentrations up to 250 μg/mL, which could favour scarless wound healing. Acute dermal toxicity studies on AgNP gel formulation in Sprague−Dawley rats displayed complete safety for topical application. These results clearly show that silver nanoparticles could supply a safer alternative to conventional antimicrobial agents in the form of a topical antimicrobial formulation.

Knetsch and Koole[130] reported that bacterial infection from medical devices is a crucial issue and accounts for an increasing number of deaths as well as high medical costs. A number of different strategies have been suggested in order to minimize the incidence of infections that are related to medical devices. One way to avert infection is by adjusting the surface of the devices in a way to prevent the occurrence of bacterial fixing. In order to achieve this, the surface has to be completely modified with mostly hydrophilic polymeric surface coatings. These materials are designed to be non-fouling, which basically implies that protein adsorption and subsequent microbial fixing are lowered. Incorporation of antimicrobial agents in the bulk material or as a surface coating is seen as a feasible alternative for systemic application of antibiotics. However, what restrains the application of antibiotics in a preventive strategy is the manifestation of more and more multi-drug resistant bacterial strains. In order to avert bacterial fixing and the subsequent formation of biofilm, silver nanoparticles have been applied on the surfaces of medical devices. The application of the nanoparticles on the device surface is achieved either through the direct deposition on the surface of the device, or alternatively, through a polymeric surface coating. This results in the slow release of silver from the surface, thereby terminating the bacteria existing near the surface. The past decade has seen the emergence of a number of studies focusing on the application of the concept of silver nanoparticles as an antimicrobial agent on a number of medical devices. What remains an issue around this concept, however, is the uncertainty that clouds the accurate antimicrobial mechanism of silver.

Bankar *et al.*[131] synthesized bio-inspired silver nanoparticles with the aid of a novel, harmless, eco-friendly biological material, the banana peel extract (BPE). Boiled, crushed, acetone precipitated, air-dried peel powder was utilized for reducing silver nitrate. Silver nanoparticles were assembled when the reaction conditions were adjusted with respect to pH, BPE content, concentration of silver nitrate and incubation temperature. The colourless reaction mixtures turned brown and displayed UV–visible spectra attributes of silver nanoparticles. Scanning electron microscope (SEM) observations revealed the predominance of silver nanosized crystallites after short incubation phases. When the reaction mixtures were incubated for 15 days, some micro-aggregates were also observed. Energy dispersive X-Ray spectrometer (EDS) studies and X-ray diffraction analysis confirmed the existence of silver nanoparticles. Fourier transform infrared spectroscopy (FTIR) displayed the role of different functional groups (carboxyl, amine and hydroxyl) in the synthetic procedure. These silver nanoparticles showed antimicrobial activity against fungal as well as bacterial cultures. The structures manufactured by the novel, cost-effective, harmless, eco-friendly, abundantly available agricultural waste material (BPE) have the ability to be applied in the fields of microelectronics, biodiagnostics, sensing, and imaging as well as in designing new drugs.

Simple green chemical routes for enhancing bactericidal coatings could be very promising for potentially environmentally friendly applications, as reported by Kumar *et al.*[132] In their work, the researchers synthesized metal nanoparticle-embedded paint through an environmentally friendly chemistry route from general household paint using just one step. Oils are known to possess a naturally occurring oxidative drying procedure that involves free-radical exchange. Without the utilization of any reducing and stabilizing agents, this mechanism was largely responsible for the reduction of metal salts and also the scattering of metal nanoparticles in the oil media. These well-scattered metal nanoparticle-in-oil dispersions can be utilized directly, akin to commercially available paints, on nearly all kinds of surfaces such as wood, glass, steel and different polymers. Coating the surfaces with silver nanoparticle-paint resulted in them displaying excellent antimicrobial properties by destroying both Gram-positive human pathogens (*S. aureus*) and Gram-negative bacteria (*E. coli*). The procedure they enhanced was very general and could find application in the synthesis of a diversity of metal nanoparticle-in-oil systems.

2.6.2. Gold Nanoparticles

The past few years have seen great progress in the fabrication of nanomaterials with potential applicability in biological, biomedical and catalytic systems. In this regard, noble metal nanoparticles have taken centre stage.[133, 134]

Gold nanoparticles are arguably the most appealing member of the noble metal nanoparticles family due to their potential applicability in fields such as nonlinear optics, surface enhanced Raman scattering, gene expression, chemical catalysis and disease diagnosis, to name a few.[135-137] Gold nanoparticles are also known for their unique and tunable surface Plasmon resonance (SPR). For gold nanospheres, the SPR occurs in the visible spectral region, at around 520 nm, which is the origin of the ruby-red colour of the nanoparticles in solution.[138]

A lot of research has over the past few years been devoted to the synthesis of gold nanoparticles with controlled sizes and shapes.

2.6.2.1. Synthesis of Gold Nanoparticles

The modern era of gold nanoparticle synthesis emerged about 150 years ago through the work conducted by Michael Faraday, who is believed to be the first to observe that colloidal gold solutions possess properties that vary from bulk gold. [139] Since this major breakthrough, a number of methods have been developed for the synthesis of gold nanoparticles with controlled sizes and shapes.

The typical synthesis of gold nanoparticles basically involves the reduction of gold salts through chemical reductants such as sodium citrate and sodium borohydride, yielding particles with sizes of 12-100 and 2-10 nm, respectively.[140] Through chemical synthetic methods, however, it is very likely that trace amounts of unreacted reagents may remain in solution, which may result to environmental pollution.

This drawback, together with the emergence of green chemistry principles and consequently, green nanotechnology, has seen research into the synthesis of gold nanoparticles slowly lean towards the use of environmental friendly methods. As a result, plant materials are slowly replacing the conventional, harsh reducing agents in the synthesis of gold nanoparticles.[141]

Das *et al*[142] reported a green synthesis method of gold nanoparticles using ethanolic leaf extract of *Centella asiatica.* In their procedure, they dried the leaves of *C. asiatica* and ground them to a fine powder and finally completed the extraction using ethanol. The nanoparticles were then synthesized by simply mixing the leaf extract with $HAuCl_4$ at room temperature. XRD analysis showed the formation of highly crystalline gold nanoparticles, whereas UV and TEM analyses showed the formation of particles in the nano-range.

In another similar study, Song *et al*[143] used leaf extracts of *Magnolia kobus* and *Diopyros kaki* to synthesize metallic gold nanoparticles. They studied the effect of the concentration of the leaves in the particle sizes of the resulting particles. They discovered that, increasing the leaf concentration results in a decrease in the particle sizes. Analytical characterization techniques confirmed the formation of highly crystalline, quality nanoparticles.

Other similar methods in which plant leaf extracts were successfully used include those used by Noruzi *et al*.,[144] in which *Rosa hybrida* petal extract was used to synthesize gold nanoparticles at room temperature; Chandran *et al*.,[145] who used *Aloe vera* plant extract to synthesize gold and silver nanoparticles; Smitha *et al*.,[146] who used *Cinnamomum zeylanicum* leaf broth; Kumar *et al*.,[147] who used *Zingiber officinale* extract; Dubey *et al*.,[148] who used *Rosa rugosa* leaf extract, to mention a few. In all these studies, the synthesis of high quality nanomaterials was accomplished, as evident from the characterization techniques employed. The use of plant extracts makes the final materials potentially applicable in various biomedical and biotechnological systems.

2.6.2.2. Application of Gold Nanoparticles in Catalysis

Catalysts are known to lower the activation energies of reactions and therefore increase the rate of reaction and the yield of the resulting products. The better understanding of the reactions and properties of nanoparticles has exponentially increased the use of nanoparticles as catalysts. Nanoparticle catalysis has been investigated for both heterogeneous and homogeneous systems.

The earliest reference to gold as a catalyst dates back to 1925, when it was used for the oxidation of carbon monoxide.[149] Since this discovery, there has been an instantaneous interest in the catalytic properties of gold nanoparticles.

Lopez *et al*.[150] studied the effects that contribute to the special catalytic properties of supported gold nanoparticles. They reported that the most important effect contributing to the

catalytic properties is related to the availability of many low-coordinated gold atoms on the small particles. They also reported the effects related to the interaction with the support to have a contribution, but to a much lesser extent.

The catalytic parameters determining the activity and selectivity of supported gold nanoparticles for the aerobic oxidation of alcohols were studied by Abad *et al*.[151] In their findings, they singled out the possibility that the activity of gold catalyst for the aerobic oxidation of alcohol involves the presence of a high density of gold atoms that have the potential to act as Lewis-sites, which coordinate with alcohols to form gold alcoholates and also accept hybrids. They reported that the role of the support should not only be to provide stability for positive gold species by interfacial gold-support interactions, but also to facilitate oxygen activation to promote the re-oxidation of metal hybrids.

Chen *et al*.[152] conducted a study in which they prepared and applied highly dispersed gold nanoparticles supported on silica in catalytic hydrogenation of aromatic nitro compounds. They prepared the nanoparticles by using organic groups, the 3-glycidoxypropyl groups, on modified silica as reductants. The prepared catalysts displayed exceptional catalytic properties for the reduction of a number of aromatic compounds to their corresponding amines by hydrogen.

In the quest to promote and maintain green chemistry principles, Aromal *et al*.[153] achieved the synthesis of gold nanoparticles by utilizing *Trigonella foenum-graecum*, and investigated their size-dependant catalytic activity. Their synthesis method, which was based on the reduction of $AuCl_4^-$ by the *Trigonella foenum-graecum* extract, was simple, economical, efficient and nontoxic. The synthesized gold nanoparticles displayed outstanding catalytic activity when tested for the reduction of 4-nitrophenol to 4-aminophenol by excess $NaBH_4$. The catalytic activity was found to be size-dependant, with smaller nanoparticles displaying faster activity than larger ones.

2.7. References

1. M.J. Hajipour, K.M. Fronm, A.K. Ashkarran, D.J. de Aberasturi, I.R. de Larramendi, T. Rojo, V. Serpooshan, W.J. Parak, M. Mahmoudi, *Trends in Biotechnol.*, 30(10), 2012, 499-511.
2. S. Barcikowski, A. Hahn, A.V. Kabashin, B.N. Chichkou, *App. Phys., A,* 87(1), 2007, 47-55.
3. C.N.R. Rao, G.U. Kulkami, P.J. Thomas, P.P. Edwards, *Chem. Eur. Journal,* 8(1), 2002, 28-35.
4. J.M. Campelo, D. Luna, R. Luque, J.M. Marinas, *ChemSusChem*, 2, 2009, 18-45.
5. X. Luo, A. Morrin, A.J. Killard, M.R. Smyth, *Electroanalysis,* 18(4), 2006, 319-326.
6. Q.A. Pankhurst, J. Conndly, S.K. Jones, J. Dobson, *J. Phy.,* 36(13), 2003, 167-181.
7. S.L.Y. Tang, R.L. Smith, M. Poliakoff, *Green Chem.,* 2005, 7, 761-762.
8. A. Galuszka, Z. Migaszewski, J. Namiesnik, *Trends in An. Chem.*, 50, 2013, 78-84.
9. H. M. Akil, M.F. Omar, A.A.M. Mazuki, S. Safiee, Z.A.M. Ishak, A. Abu Bakar, *Mater. Des.,* 32, 2011, 4107-4121.
10. J.R. Barone. W.F. Schmidt, *Comp. Sci. and Technol.*, 65,2005, 173-181
11. P. Wambua, J. Ivens, I. Verpoest, *Comp. Sci. and Technol.,* 63(9), 2009, 1259-1264.
12. A.K. Bledzki, J. Gassan. *Prog. Polym. Sci.*, 24, 1999, 221-274.
13. T. Folster, W. Michaeli, *Kunstoffe Germ. Plas.,* 83(9), 1993, 687-691.
14. M. Jonoobi, R. Oladi, Y. Davoudspour, K. Oksman, A. Dufresne, Y. Hamzeh, R. Davoodi, *Cellulose*, 22, 2015, 935-969.
15. A. Heredia, A. Jimenez, R. Guillen, *Z. Lebensm. Unters. Forch.,* 200, 1995, 24-31.
16. H. Ku, H. Wang, N. Pattarachaiyakoop, M. Trada, *Comp. Part B,* 42(4), 2011, 856-873.
17. G. Bogoeva-Caceva, M. Avella, M. Malinconico, A. Buzarovska, A. Grozdanov, G. Gentile, M.E. Errico, *Polym. Comp.,* 11(1), 2007, 99-107.
18. D. N. Saheb, J.P. Jog, *Adv. Polym. Technol.,* 49, 1999, 1253-1272.
19. S.N. Walford, P.G. M. du Boil, *Proc. S. Afr. Sug. Technol. Ass.,* 80, 2006, 39-61.
20. C.C. Ripoli, Molina Jr., M.L.C. Ripoli *Sci. Agric.,* 57, 2000, 677-681.
21. S. Thorsell, F.M. Epplin, R.L. Huhnke, C.M. Taliaferro, *Biomass and Bioenergy*, 27, 2004, 327-337.
22. P. McKendry, *Biores. Technol.,* 83, 2002, 47-54.
23. A. Pandey, C.R. Soccol, P. Nigam, V.T. Soccol, *Biores. Technol.,* 74(1), 2000, 69-80.

24. M.J. Taherzadeh, K. Karmi, *Int J. Mol. Sci.*, 9, 2008, 1621-1651.
25. M. Laser, D. Schulman, S.G. Allen, J. Lichwa, M.J. Antal Jr., L.R. Lynd, *Bioresour. Technol.*, 81, 2002, 33-44.
26. M.E. Himmel, S.Y. Ding, D.K. Johnson, W.S. Adney, M.R. Nimlos, J.W. Brady, T.D. Foust, *Science*, 315, 2007, 804-807.
27. Y.P. Zhang, L.R. Lynd, *Biotechnol. Bioeng.*, 88, 2004, 797-824.
28. A.C. O'sullivan, *Cellulose*, 4(3), 1997, 173-207.
29. D. Bhattacharya, L.T. Germinario, W.T. Winter, *Carb. Polym.*, 73(3), 2008, 371-377.
30. M. Roman, S. Dong, A. Hirani, Y.W. Lee, *Polysacch. Mater.*, 4017(4), 2009, 81-91.
31. E. Lam, K.B. Male, J.H. Chong, A.C.W. Leung, J.H.T. Luong, *Trends in Biochem.*, 30(5), 2012, 283-291.
32. V. Incani, C. Danumah, Y. Boluk, *Cellulose*, 20(1), 2013, 191-200.
33. Y. Zhou, C. Fuentes-Hernandez, T.M. Khan, J.C. Liu, J. Hsu, J.W. Shim, A. Dindar, J.Y. Youngblood, R.J. Moon, B. Kippelen, *Sci. Rep.*, 3(1536), 2013, 1-5.
34. R.J. Moon, A. Martini, J. Nairn, J. Simonsen, J. Youngblood, *Chem. Soc. Rev.*, 40, 2011, 3941-3994.
35. L.A. Sacui, R.C. Nieuwendaal, D.J. Burnett, S.J. Stranick, M.Jorfi, C. Weder, E.J. Foster, R.T. Olsson, J.W. Gilman, *ACS Appl. Mater. Interfaces*, 6(9), 2014, 6127-6135.
36. Y. Habibi, L.A. Lucia, O.J. Rojas, *Chem. Rev.*, 110(6), 2010, 3479-3500.
37. P. Lu, Y.L. Hsieh, *Carb. Polym.*, 82(2), 2010, 329-336.
38. D. Klemm,F. Kramer, S. Moritz, T. Lindstrom, M. Ankerfors, D. Gray, A. Dorris, *Angew. Chem. Int. Ed.*, 50, 2011, 5438-5466.
39. D. Bondeson, A. Mathew, K. Oksman, *Cellulose*, 13, 2010, 171-180.
40. A.C.W. Leung, S. Hrapovic, E. Lam, Y. Liu, K.B. Male, K.A. Mahmoud, J.H.T. Luong, *Small*, 7(3), 2011, 302-305.
41. M. Grunert, W.T. Winter, *Journal of Polym. and the Environ.*, 10(1-2), 2002, 27-30.
42. J. A. Diaz, X. Wu, A. Martini, J.P. Youngblood, R.J. Moon, *Biomacromol.*, 14(8), 2013, 2900-2908.
43. M. Hasani, E.D. Cranston, G. Westman, D.G. Gray, *Soft Matter*, 4, 2008, 2238-2244.
44. J. Zhang, N. Jiang, Z. Dang, T.J. Elder, R.J. Ragauskas, *Cellulose*, 15, 2008, 489-496.
45. Y. Habibi, A.L. Goffin, N. Schiltz, E. Duquense, P. Dubois, A. Dufresne, *J. Mater. Chem.*, 18, 2008, 5002-5010.

46. A. Pei, Q. Zhou, L.A. Berglund, *Comp. Sci. and Technol.,* 70(5), 2010, 815-521.
47. X. Wang, H. Li, Y. Cao, G. Tang, *Biores. Technol.,* 102, 2011, 7957-7965.
48. V. Landry, A. Alemdar, P. Blachet, *Forest prod. J.,* 61, 2011, 104-112.
49. S.M.L. Rosa, N. Rehman, M.I.G. de Miranda, S.M.B. Nachtigall. C.I.D. Bica, *Carb. Polym.* 87, 2012, 1131-1138.
50. A. Mandal, D. Chakrabarty, *Carb. Polym.,* 86, 2011, 1291-1299.
51. A. Kumar, Y. Singh Negi, V. Chadhary, N. Kant Bhardwaj. *Journ. Mat. Phys. And Chem.* 2, 2014, 1-8.
52. F.W. Herrick, R.L. Casebier, J.K. Hamilton, K.R. Sandberg, *J. Appl. Polym. Sci.,* 37, 1983, 797-813.
53. A.F. Turbak, F.W. Snyder, K.R. Sandberg, *J. Appl. Polym. Sci.,* 37, 1983, 815-827.
54. J. Zhang, T.J. Elder, Y. Pu, A.J. Ragauskas, *Carb. Polym.,* 69(3), 2007, 607-611.
55. R. Hashaikeh, H. Abushammala, *Carb. Polym.,* 83(3), 2011, 1088-1094.
56. J. Li, X. Wei, Q. Wang, J. Chen, G. Chang, L. Kong, J. Su, Y. Liu, *Carb. Polym.,* 90, 2012, 1609-1613.
57. A. Alemdar, M. Sain, *Comp. Sci. and Technol.,* 68, 2008, 557-562.
58. C. Jose Chirayil, L. Mathew, S. Thomas, *Rev. Mater. Sci.,* 37, 2014, 20-28.
59. A. Llorens, E. Llorent, P.A. Picouet, R. Trboojevic, A. Fernandez, *Trends in Food Sci. and Technol.,* 24, 2012, 19-29
60. P. Gong, H. I, X. He, K. Wang, J. Hu, W. Tan, S. Zhang, X. Yong, *Nano.*,18, 2007, 5-9.
61. P.S. Schabes-Retchkiman, G. Canizal, R. Herrera-Becerra, C. Zorilla, H.B. Liu, J.A Ascencio, *Optic. Mater.,* 29(1), 2006, 95-99.
62. H. Gu, P.H.E. Tong, L. Wang, B. Xu, *Nano. Lett.,* 3(9), 2003, 1261-1263.
63. Z. Ahmad, R. Pandey, S. Sharma, G.K. Khuller, *Ind. J. Chest Dis. Allied Sci.,* 48, 2005, 171-176.
64. J. H. Han, *Plast. Films in Food Pack.,* 1(1), 2013, 151-180.
65. P. Appendini, J.H. Notchkiss, *Innov. Food Sci. and Emerg. Technol.,* 3, 2002, 113-126.
66. H. Lara, N.V. Ayala-Nunez, L. Ixtepan-Turrent, C. Rodriguez-Padilla, *J. Nanobiotechnol.,* 8(1), 2010, 4-10.
67. X. Chen, H.J. Schluesener, *Toxicol. Lett.,* 176(1), 2008, 1-12.

68. A.S. Kazachenko, A.V. Legler, O.V. Peryanova, Y.A. Vstavskaya, *J. Pharm. Chem.*, 34(5), 2000, 257-258.
69. M.L. Gulrajani, D. Gupta, S. Periyasamy, S.G. Muthu, *J. App. Polym. Sci.*, 108, 2008, 614-623.
70. G.A. Martinez-Castanon, N. Nino-Martinez, F. Martinez-Guterrez, J.R. Martinez-Mendoza, F. Ruiz, *J. Nanopart. Res.*, 10, 2008, 1343-1348.
71. A. Panacek, L. Kvitek, R. Prucek, M. Kolar, R. Vecerova, N. Pizurova, V.K. Sharma, T. Nevecna, R. Zboril, *J. Phys. Chem. B*, 110(3), 2006, 16248-16253.
72. A. Schneider, W. Oppliger, P. Jenno, *J. Biol. Chem.*, 269(12), 1994, 8635-8638.
73. C.S. Sharma, R.K. Nema, V.K. Sharma, *Stan. J. Pharm. Sciences*, 2(2), 2009, 42-47.
74. S.B. Long, X. Tao, E.B. Campbell, R. Mackinnon, *Nat. Int. J. Sci.*, 450, 2007, 376-382.
75. P. Mahapatra, K. Shibuya, A.D. Lopez, F. Coullare, F.C. Notzon, C. Rao, S. Szreter, *Lancet*, 370(10), 2007, 1653-1663.
76. G. Zeng, B. Huang, S.P. Neo, J. Wang, M. Cai, *Mol. Biol. Cell.*, 18(12), 2007, 4885-4898.
77. R. Sanghi, P. Verma, *Biores. Technol.*, 100(1), 2009, 501-504.
78. J. Kasthuri, S. Veerapandian, N. Rajendiran, *Colloids Surf. B*, 68, 2009, 55-60.
79. S.S. Shankar, A. Ahmad, M. Sastry, *Biotechnol. Prog.*, 19, 2003, 1627-1631.
80. J.Y. Song, B.S. Kim, *Bioprocess Biosyst. Eng.*, 32(1), 2009, 79-84.
81. A. Ahmad, P. Mukherjee, S. Senapati, D. Mandal, M.I. Khan, R. Kumal, *Colloids Surf. B*, 28, 2003, 313-318.
82. S. Stoeva, K.J. Klabunde, C.M. Sorensen, I. Dragieva, *J. Am. Chem. Soc.*, 124(10), 2002, 2305-2311.
83. C. Marambio-Jonenes, E.M.V. Hoek, *J. Nanopart. Res.*, 12, 2010, 1531-1551.
84. A. Grigor'eva, I. Saranina, N. Tikunova, A. Safonov, N. Timoshenko, A. Rebrov, E. Ryabchikova, *Biometals*, 26(3), 2013, 479-488.
85. J.L. Castro-Mayorga, A. Martinez-Abud. M.J. Fabra, C. Olivera, M. Reis, J.M. Lagaron, *Int. J. Bio. Macromol.*, 71, 2014, 103-110.
86. M. Moritz, M. Geszke-Moritz, *J. Chem. Eng.*, 228, 2013, 596-613.
87. U. Damm, J.H.G. Woudenberg, P.F. Cannon, P.W. Crous, *Fung. Div.*, 39, 2009, 45-87.

88. E.G. Neal, H. Chaffe, R.H. Schwartz, M.S. Lawson, N. Edwards, G. Fitzsimmons, A. Whitney, J.H. Gross, *Lancet Nuerol,* 6, 2008, 500-506.
89. P. Dibrov, J. Dzioba, K.K. Gosink, C.C. Hase, *Antimicro. Agents Chemother.,* 46, 2002, 2668-2671.
90. M. Yamanka, K. Hara, J. Kudo, *Appl. Environ. Microbiol.,* 71, 2005, 7589-7593.
91. Q.L. Feng, J. Wu, G.Q. Chen, F.Z. Cui, T.N. Kim, J.O. Kim, *J. Biomed. Mater. Res.,* 52(4), 2000, 662-668.
92. K.I. Batarseh, *J. Antimicrob. Chemother.,* 20, 2004, 546-551.
93. L. Li, C. Zhao, Y. Zhang, J. Yao, W. Yang, Q. Hu, C. Wang, C. Cao, *Food Chem.,* 215, 2017, 477-482.
94. S.D.F. Mihindukulasuriya, L.T. Lim, *J. Food and Drug Anal.,* 40(2), 2014, 149-167.
95. T.I. Radsin, I.S. Ristic, B.M. Pilic, A.R. Novakovic, *Antimicrob. Nanomater. for Food Pack. App.,* 43(2), 2016, 119-126.
96. H. Kong, J. Jang, *Lanmuir*, 24, 2008, 2051-2055.
97. X. Li, Y. Xing, Y. Jiang, Y. Ding. W. Li, *Int. J. Food Sci. and Technol.,* 44, 2009, 2161-2168.
98. J. An, M. Zhang, S. Wang, J. Tang, *J. Food Sci. and Technol.,* 41, 2008, 1000-1007.
99. A. Emamifar, M. Kadivar, M. Shahedi, S. Soleimanian-Zad, *Innov. Food Sci. and Emerg. Technol.,* 3, 2010, 742-748.
100. M.A. Del Nobile, M. Cannarsi, C. Altieri, M. Snigaglia, P. Favia, G. Iacoviello, *J. Food Sci.,* 6, 2004, 379-383.
101. S. Mahanty, R. Parida, A. Kuanar, S. Sahoo, S. Nayak, *J. Med. Plants Res.,* 6(16), 2012, 1-5.
102. K. Vimala, Y.M. Mohan, K.S. Sivudu, K. Varaprasad, S. Ravindra, N.N. Reddy, *Colloids and Surf. B,* 76, 2010, 1248-1258.
103. J.W. Rhim, L.F. Wang, S.I. Hong, *Food Hydrocol.,* 33(2), 2013, 327-335.
104. K.P. Bankara, D. Maity, M.M.R. Mollick, D. Mandal, B. Bhowmick, M.K. Bain, A. Chakraborty, J. Sankar, K. Acharya, D. Chattopadhyay, *Carb. Polym.,* 89(4), 2012, 1159-1165.
105. A. Pandey, H. Yoon, E.R. Lyver, A. Dancis, D. Pain, *Mitochon.,* 12(5), 2012, 539-549.
106. S.Y. Seo, G.H. Lee, S.H. G. Lee, S.Y. Jung, J.O. Lim, J.H. Choi, *Carb. Polym.,* 90(1), 2012, 109-115.

107. M. Turalija, S. Bishof, A. Budimir, S. Gaan, *Comp. Part B,* 102, 2016, 94-99.

108. P. Gong, H. Li, X. He, K. Wang, J. Hu, W. Tan, S. Zhang, X, Yang, *Nanotech.,* 18(28), 2007, 5-9.

109. P. Jain, T. Pradeep, *Biotechnol. Bioeng.*, 91(1), 2005, 59-63.

110. R. Prucek, J. Tucek, M. Kilianova, A. Panacek, L. Kvitek, J. Filip, M. Kokar, K. Tomankova, R. Zboril, *Biomater.*, 32, 2011, 4704-4713.

111. M. Sureshkumar, D.Y. Siswanto, C.K. Lee, *J. Mater. Chem.,* 20, 2010, 6948-6955.

112. A. Orsuwan, S. Shankar, L.F. Wang, R. Sothornvit, J.W. Rhim, *J. Food Sci. Technol.,* 60, 2016, 476-485.

113. L.K. Krehula, A. Papic, S. Krehula, V. Gilja, L. Foglar, Z. Hrnjak-Murgik, *Polym. Bulletin*, 8, 2016, 1-18.

114. P. Kanmani, J.W. Rhim, *Food Chem.*, 148, 2014, 162-169.

115. M.C. Siqueira, G. F. Coelho, M.R. de Moure, J.D. Bresolin, S.Z. Hubinger, J.M. Marconcini, L.H.C. Mattoso, *J. Nanosci. and Nanotech.,* 14(7), 2014, 5512-5517.

116. M. Eslami, M. Bayat, A.S.M. Nejad, A. Sabokbar, A.A. Anvar, *Saudi J. Bio. Sci.,* 23(3), 2016, 341-347.

117. A.A. Becaro, F.C. Puti, A.R. Panosso, G.C. Gern, H.M. Bradao, D.S. Correa, M.D. Ferreira, *Food and Bioproc. Technol.,* 9(4), 2016, 637-349.

118. J.L. Castro Mayorga, M.J. Fabra, A.M. Pourrahimi, R.T. Olsson, J.M. Lagaron, *Food and Bioprod. Process.,* 101, 2017, 32-44.

119. R.J.B. Pinto, P.A.A.P. Marques, C.P. Neto, T. Trindade, S. Daina, P. Sadocco, *Acta Biomater.,* 5(6), 2009, 2279-2289.

120. A. Fernandez, E. Soriano, G. Lopez-Carballo, P. Picouet, E. Lloret, R. Gavara, P. Hernandez-Mumoz, *Food Res. Int.*, 42, 2009, 1105-1112.

121. A. Fernandez, P. Picouet, E. Lloret, *Int. J. Food Microbiol.,* 142(1-2), 2010, 222-228.

122. M.R. de Moura, L.H.C. Mattoso, W. Zucolotto, *J. Food Eng.,* 109, 2012, 520-524.

123. M. Rai, A. Yadav, A. Gade, *Biotech. Adv.*, 27(1), 2009, 76-83.

124. S. Ahmed, A. Ahmad, B.L. Swami, S. Ikram, *J. Adv. Res.,* 7(1), 2016, 17-28.

125. X.L. Cao, C. Cheng, Y.L. Ma, C.S. Zhao, *J. Mater. Sci.: Mater. and Med.,* 21(10), 2010, 2861-2868.

126. T. Maneerung, S. Tokura, R. Rujiravanit, *Carb. Polym.,* 72(1), 2008, 43-51.

127. C.A. Impellitteri, T. M. Tolayamat, K.G. Scheckel, *J. Environ. Qual.,* 38, 2009, 1528-1530.

128. D. Roe, B. Karadikar, N. Bonn-Savage, B. Gibbins, J.P. Roullet, *J. Antimicrob. Chemother.,* 61(4), 2008, 869-879.

129. J. Jain, S. Arora, J.M. Rajwade, P. Omray, S. Khandlwal, K.M. Paknikar, *Mol. Pharma.,* 6(5), 2009, 1388-1401.

130. M.L.W. Knetsch, L.H. Koole, *Polym.,* 3(1), 2011, 340-366.

131. A.Bankar, B. Joshi, A.R. Kumar, S. Zinjarde, *Colloids and Surf. A: Physiochem. Eng. Asp.,* 368,2010, 58-63.

132. A. Kumar, P.K. Vemula, P.M. Ajay, G. John, *Nat. Mater.,* 7, 2008, 236-241.

133. J. Zhang, F.H.B. Lima, M.H. Shao, K. Sasaki, J.X. Wang, J. Hanson, R.R. Adzic, *J. Phys. Chem.,* 109(48), 2005, 22701-22704.

134. T.K. Sau, A.L. Rogach, F. Jackel, T.A. Klar, J. Feldman, *Adv. Mater.,* 22, 2010, 1805-1825.

135. N.L. Rosi, D.A. Giljohann, C.S. Thaxton, A.K.R. Lytton-Jean, M.S. Han, C.H. Mirkin, *Science,* 312, 2006, 1027-1050.

136. K. Kneipp, A.S. Haka, H. Kneipp, B. Baolizadegan, N. Yoshizawa, C. Boone, K.E. Shafer-Peltier, J.T. Metz, R.R. Dasapri, M.S. Feld, *App. Spectro.,* 56(2), 2002, 150-154.

137. A.J. Mieszawska, W.J.M. Mulder, Z.A. Fayad, D.P. Cormode, *Mol. Pharma.,* 10(3), 2013, 831-847.

138. I.H. El-Sayed, X. Huang, M.A. El-Sayed, *Nano. Lett.,* 5(5), 2005, 829-834.

139. G.F. Paciotti, D.G.I. Kingston, L. Tamarkin, *Drug Develop. Res.,* 67, 2006, 67-54.

140. I. Ojea-Jimenez, F.M. Romero, N.G. Bastus, V. Puntes, *J. Phys. Chem. C,* 144(4), 2010, 1800-1804.

141. A.K. Mittal, Y. Chisti, U.C. Manerjee, *Biotech. Adv.,* 31(2), 2013, 346-356.

142. R. K. Das, B.B. Borthakur, U. Borra, *Mater. Lett.,* 64, 2010, 1445-1447.

143. J.Y. Song, H.K. Jang, B.S. Kim, *Proc. Biochem.,* 44, 2009, 1133-1138.

144. M. Noruzi, D. Zare, K. Khoshnevisan, D. Davoodi, *Spectrochimica Acta,* 79, 2011, 1461-1465.

145. S.P. Chandran, M. Chauhdhary, R. Pasricha, A. Ahmad, M. Sastry, *Biotechnol. Prog.*, 22, 2006, 577-583.

146. S.L. Smitha, D. Philip, K.G. Gopchandran, *Spectrochimica Acta,* 74(3), 2009, 735-739.

147. K.P. Kumar, W. Paul, C.P. Sharma, *Proc. Biochem.*, 46(10), 2011, 2013-2017.

148. S.P. Dubey, M. Lahtinea, M. Sillanpaa, *Colloids and Surf. A,* 364(1-2), 2010, 34-41.

149. W.A. Bone, G. W. Andrew, *Proc. Roy. Soc. A, 109, 1925, 409.*

150. N. Lopez, T.V.W. Janssens, B.S. Clausen, Y. Xu, M. Mavrikakis, T. Bligaard, J.K. Norskov, *J. Catal.*, 223, 2004, 232-235.

151. A. Abad, A. Corma, H. Garcia, *Chem. Eur. Journ.*, 14, 2008, 212-222.

152. Y. Chen, J. Qiu, X. Wang, J. Xiu, *J. Catal.*, 242, 2006, 227-230.

153. S.A. Aromal, D. Philip, *Spectrochimica Acta*, 97, 2012, 1-5.

CHAPTER THREE:

EXTRACTION AND CHARACTERIZATION OF CELLULOSE FROM SUGARCANE BAGASSE

3.1. Introduction

The extraction of cellulose from its natural matrix in plants involves the removal of lignin, hemicelluloses and pectins. Over the past few years, many methods have been suggested and used by different researchers to extract cellulose from different plants.[1-17] The methods generally involve basic or oxidative treatments that have the ability to discharge cellulose. Alternatively, treatment with peracids has been used to extract cellulose. This step is significant due to the fact that it has the ability to change the chemical and thermal stability of cellulose as well as the crystalline organization and polymorphism of the material. Other researchers used an acid-induced destructuring process, during which the heterogeneous acid hydrolysis involves the diffusion of acid molecules into cellulose fibres, followed by cleavage of glycosidic bonds. That was followed by centrifugation, dialysis and ultrasonication.[18] Most studies used six steps, which were the pre-treatment of the fibres with sodium hydroxide, hydrogen peroxide, sodium hydroxide and $Na_2B_4O_7.10H_2O$, HNO_3 and HAc, ethanol, water and finally drying the product in an oven until constant weight. Other researchers involved the treatment of fibres with sodium chlorite which facilitated the removal of lignin, which was followed by NaOH and drying until constant weight.[19] Although both methods resulted in cellulose with significant quantities of hemicelluloses or lignin, the first procedure was less environmentally aggressive, while the second involved less process time and drove to fibres with more homogeneous diameter distribution.

Treatments consisting of alkali extraction and bleaching have been the mostly used in the extraction of cellulose.[20, 21] The alkali extraction treatment allows the removal of soluble polysaccharides, and the subsequent bleaching treatment removes most of the residual phenolic molecules like lignin or polyphenols.

There are various methods used to extract cellulose; nonetheless the literature is virtually mute about a methodical comparison of properties from different methods and possible benefits for different applications. Five different methods of extraction of cellulose from the same sugar cane bagasse were used in this study. Characterization techniques used for comparison included TGA, FTIR, XRD, OM, and SEM.

3.2. Experimental

3.2.1. Materials

Sugarcane bagasse was obtained from a sugarcane mill in Felixton near Empangeni, South Africa. Acetic acid was obtained from Laboratory Consumables and Chemical Suppliers, sodium sulphite and sodium hydroxide were obtained from Merk, sodium chlorite was obtained from Sigma Aldrich, and sodium hypochlorite was obtained from a local supermarket. All chemicals were used without further purification, but were prepared to the desired concentrations.

3.2.2. Cleaning of bagasse

Sugarcane bagasse was obtained directly from the sugar mill and was therefore very muddy. As a result, the bagasse was firstly washed thoroughly with adequate water for four times and then allowed to dry in air.

3.2.3. Extraction of cellulose from sugarcane bagasse

A total of five different methods were used for the extraction of cellulose from sugarcane bagasse.

3.2.3.1. Method 1

Sugarcane bagasse was boiled in water (4 hrs). After that it was soaked in 4 % sodium hydroxide (4hrs), followed by treating with 4 % sodium hypochlorite (commercial jik) and 2 % sodium hydroxide (4 hrs) at 100 ºC before washing with distilled water to a neutral pH. The final product was dried at room temperature for 2 days.

3.2.3.2. Method 2

From method 1, 4 % of sodium hypochlorite was acidified with acetic acid to pH4.

3.2.3.3. Method 3

From method 1, 2 and 1% of NaOH was used in the second and last step, respectively. 0.7 % sodium chlorite acidified with acetic acid to pH4 was used instead of 4 % sodium hypochlorite.

3.2.3.4. Method 4

From method 3, the last step was eliminated.

3.2.3.5. Method 5

From method 3, an additional step was added after the sodium chlorite step, in which the sample was treated with 5 % sodium sulphite at 100 ºC for three hours.

3.2.4. Characterization

3.2.4.1. Optical Microscopy (OM)

The optical microscope images of the samples were viewed using a LEICA MC 120 HD microscope. Dark and bright field modes were used to capture the images at a magnification of 40 x/ 0.65.

3.2.4.2. Scanning Electron Microscope (SEM)

The SEM measurements of the materials were performed on a Philips XL 30 FEG (at 10 kV) and DX4 detector (at 20 kV), respectively. The films were carbon-coated by using Edward's E306A coating system, prior to the analyses.

3.2.4.3. Fourier Transform Infrared (FTIR)

Infrared spectra of the samples were recorded on a Bruker FT-IR Tensor 27 spectrophotometer equipped with a standard ATR crystal cell detector. The spectra were recorded at a wavenumber range of 500-4000 cm^{-1}.

3.2.4.4. X-Ray Diffraction (XRD)

The diffraction patterns of the cellulosic materials were investigated at room temperature using an Advanced Bruker AX D8 diffractometer in the range $2\theta = 10 – 90$ º, equipped with nickel-filtered Cu *Kα* radiation ($\lambda = 1.542$ Å) at 40 kV and 40 mA. The scan speed was 0.5 sec/step.

3.2.4.5. Thermogravimetric Analysis (TGA)

Thermogravimetric analyses were carried out using a Perkin Elmer Pyris 6 TGA equipped with a closed perforated pan at a heating rate of 10 ºC/min. Approximately 2 mg of each sample was heated from 30 - 600 ºC under N_2 gas flow rate of 10 mL/min.

3.3. Results and discussion

3.3.1. Optical Microscopy

Optical microscope images of all the methods are shown in Figure 3.1 (a-e), where a-e represents results for methods 1-5, respectively. The fibres of methods 1 and 2 are agglomerated. In method 1 the fibres are more agglomerated and closely packed than in method 2. Methods 3, 4 and 5 show defibrillation and thinning of fibres, which signals the removal of non-cellulosic components in SCB. The thinning and defibrillation is further noted for the fifth method.

For the first method (Figure 3.1a), the use of sodium hypochlorite can be seen to have limited defibrillation. This is because sodium hypochlorite is highly basic in nature and therefore could not effectively facilitate the digestion of the cell walls which is meant to make the treatment with alkali more effective. The introduction of acetic acid in sodium hypochlorite in method 2 (Figure 3.1b) shows to have increased the defibrillation, but to a minor extent.

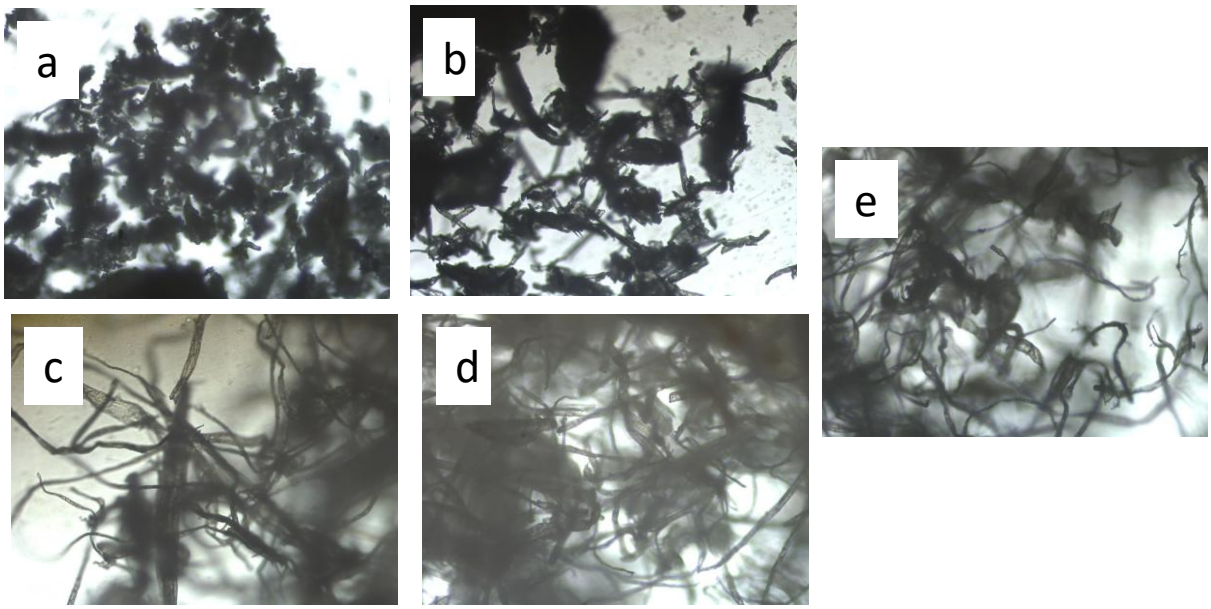

Figure 3.1: OM images of methods 1(a), 2(b), 3(c), 4(d), and 5(e).

In methods 3, 4 and 5 (Figure 3.1 c-e) acidified sodium chlorite was used for the digestion of the cell walls of SCB. This proved to be more effective than the use of sodium hypochlorite, be it acidified or not. The further thinning and defibrillation noted for the fifth method (Figure 3.1e) can be attributed to the fact that sodium sulphite was used to dissolve

the lignin-chlorine complex that forms during the digestion process. This step also helps in the removal of non-cellulosic components to some extent.

3.3.2. SEM

Figure 3.2 shows SEM micrographs of raw sugarcane bagasse, with (a) showing the general view of the fibres and pith, and (b) an amplified individual fibre. It is seen in (a) that there are many non- fibrous components scattered over the surface of the fibres. The surface of the fibres is very congested and smooth, as shown in (b). The congestion and smoothness are due to the presence of extractives such as waxes, pectins, oils and hemicelluloses. The fibres have bigger sizes and appear to be composed of many microfibrils.

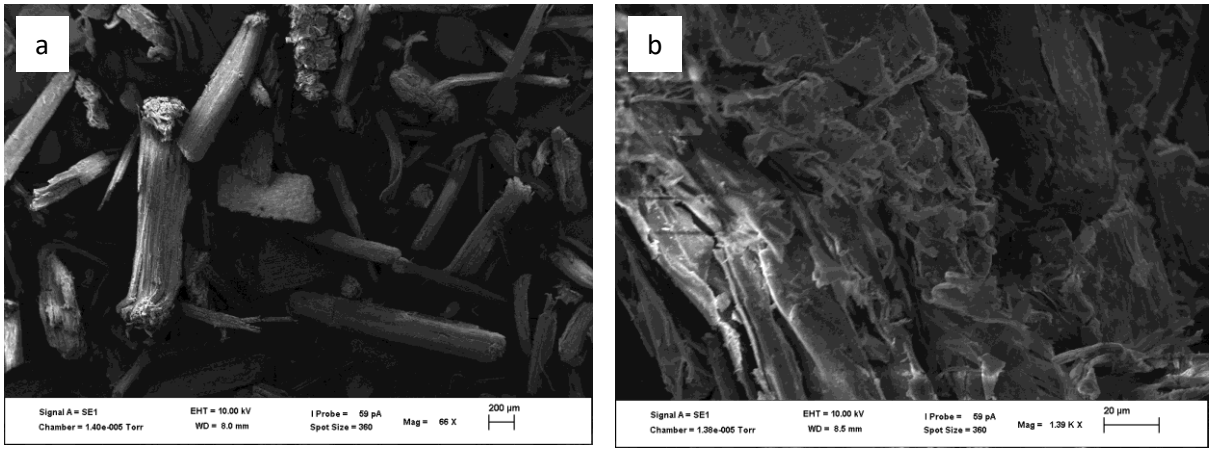

Figure 3.2: SEM micrographs of raw sugarcane bagasse

The SEM micrographs of the cellulose obtained through the different extraction methods from sugarcane bagasse are shown in Figures 3.3, 3.4 and 3.5 below.

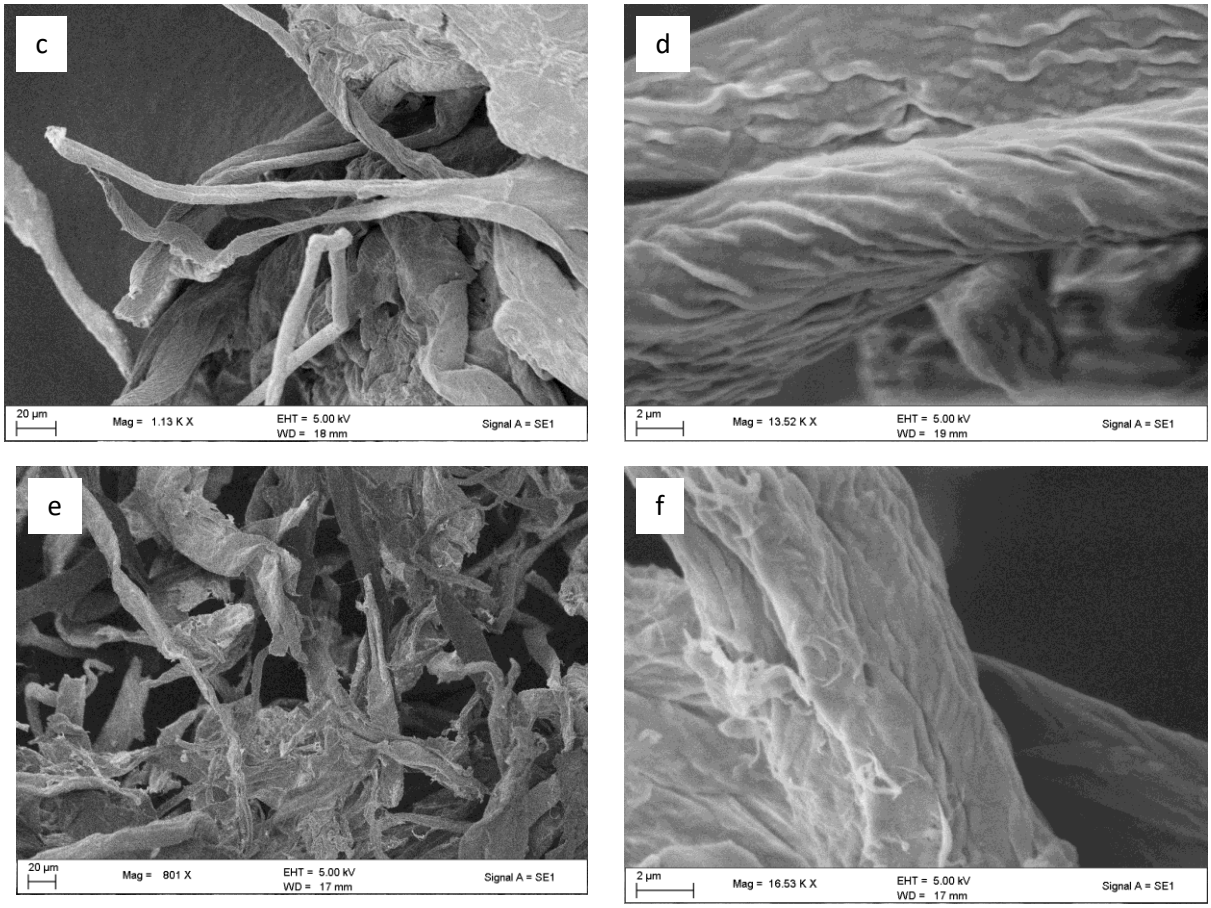

Figure 3.3: SEM micrographs of cellulose extracted from sugarcane bagasse through method 1 (c, d) and method 2 (e, f)

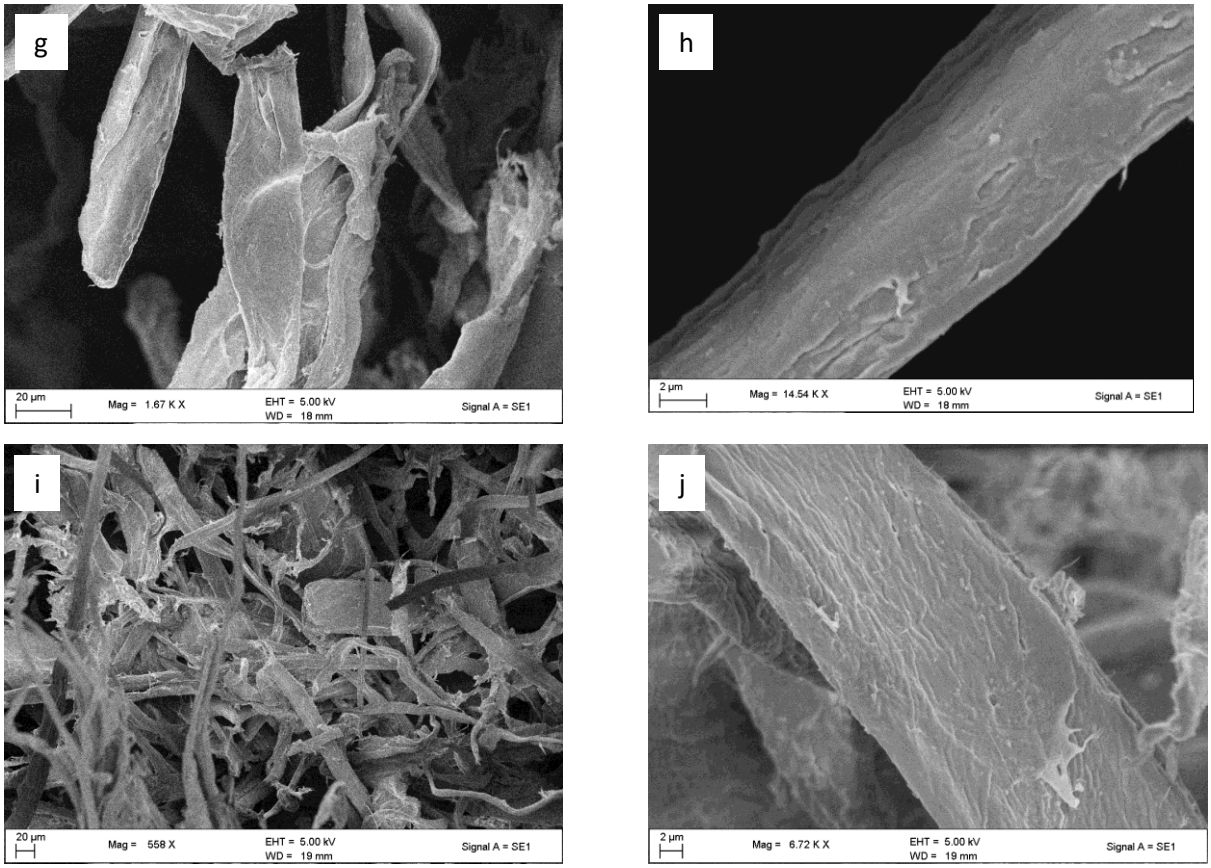

Figure 3.4: SEM micrographs of cellulose extracted from sugarcane bagasse through method 3(g, h) and method 4 (i, j).

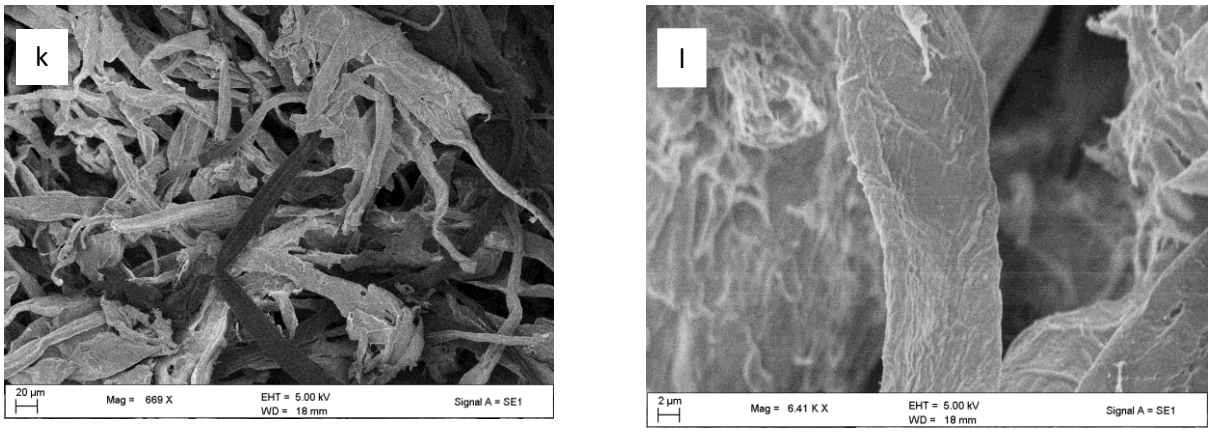

Figure 3.5: SEM micrographs of cellulose extracted from sugarcane bagasse through method 5.

The surfaces of all the cellulosic materials are cleaner and a slightly rougher in comparison to those of raw bagasse. Furthermore, individual fibres show a decrease in diameter. These factors signify the removal of hemicelluloses, lignin, pectins and waxes.

As the bagasse is treated with different chemicals, the non-cellulosic components are hydrolyzed and become water soluble. As a result, the fibrils are defibrillated, which cause thinning or reduction of their diameters, and also the dispersion of fibre bundles into individual fibres. As evident from other analyses, the fifth method shows to have the most stable and pure cellulose. SEM results are in correspondence with observations made from the optical microscopy analysis.

3.3.3. FTIR

Figure 3.6 represents FTIR spectra of the extracted cellulosic materials. For all the samples, the FTIR spectra show an O-H stretching broad band at 3500-3200 cm^{-1}, characteristic for cellulosic materials. The spectra also show C-H stretching vibration at around 2894 cm^{-1}, which is also characteristic for cellulosic materials. Absorbance peaks around 1649-1641 cm^{-1} are a result of the O-H bending of the adsorbed water. The peaks around 1054 cm^{-1} are due to the C-O-C pyranose ring stretching vibration. Another important absorption band is at around 902 cm^{-1} which is associated with the ß-glycosidic linkages between glucose.

The product of M1 reveals low O-H stretching band compared to the rest, except for M3 which shows the lowest. Furthermore, it reveals an aromatic peak at 1597 cm^{-1}, whereas for other methods the peaks are reflected at around 1640 cm^{-1}. The O-H stretching band for the product of M2 is more intense than that of the other methods. Furthermore, the product of M2 does not show a peak at 1250 cm^{-1} which is also in contrast to the other methods. As for M3, most of the aromatic peaks (e.g. 1197 cm^{-1}) have almost disappeared. M4 and M5 followed the same trend of M3, even though their peaks are slightly intense than M3 including O-H stretching.

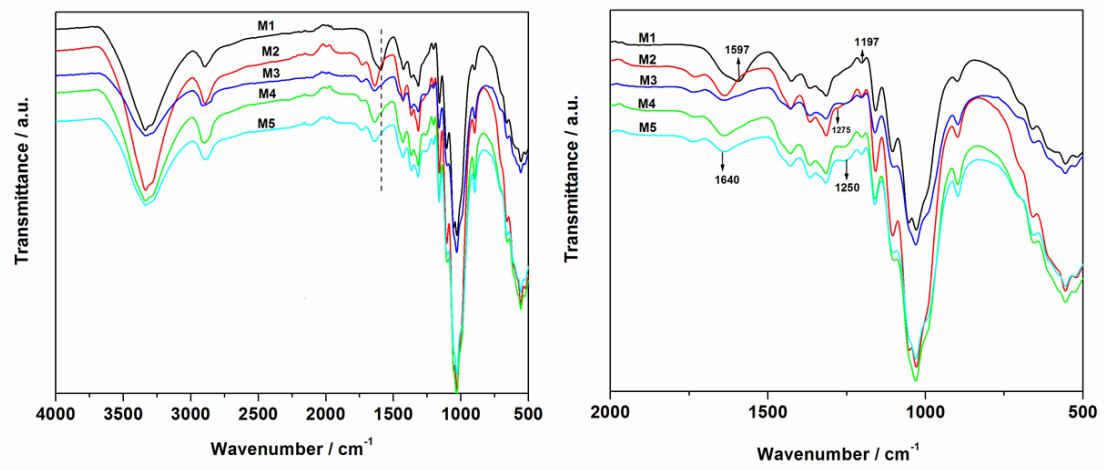

Figure 3.6: FTIR spectra of the cellulose extracted from sugarcane bagasse through the five methods.

3.3.4. XRD

Figure 3.7 shows the XRD diffractograms of the cellulose materials extracted through the five methods. All the diffractograms of the five methods display very well-defined peaks at around 2θ = 12.5 º (for 110 planes) and 2θ = 22.5 º (for 200 planes), which are representative of a typical cellulose structure. However, M1 and M2 reveal impurities which seem to have little and/no relation to the structure of cellulose. The same is apparent for the reflection at approximately 2θ = 61 º for M4 and M5. These indicate either the formation or the presence of cellulose derivatives from the chlorite salts.

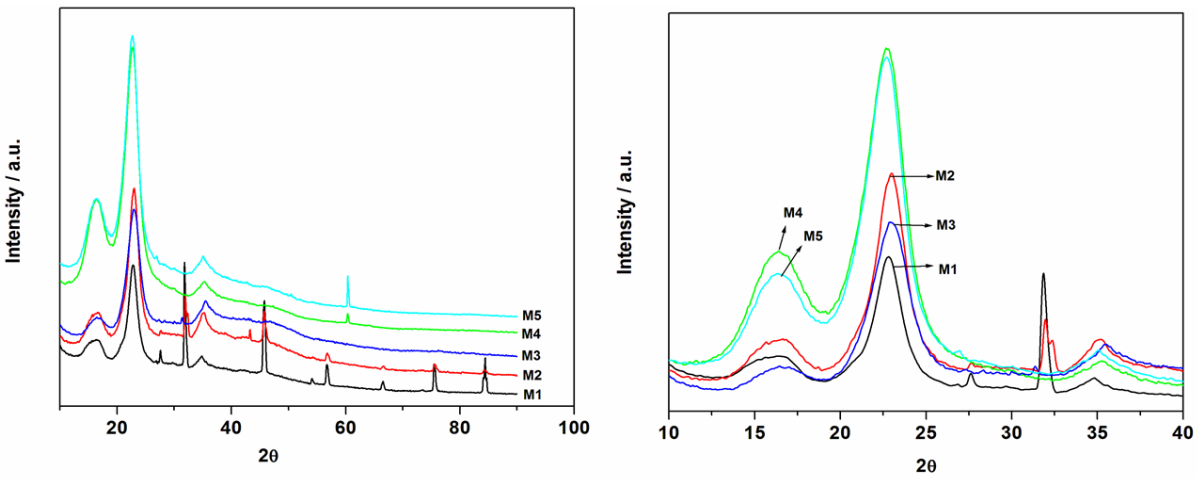

Figure 3.7: XRD diffractograms of the cellulose obtained from bagasse through the five extraction methods.

Furthermore, M4 and M5 dominated all with crystallinity index followed M2, M3 and M1 (Table 2). The formation of some cellulose derivatives is known to destruct the initial crystallinity. If that applies in the current study, it means that the use of NaOH after the chlorite salts in M1, M2 and M3 promoted the formation of cellulose derivatives which rendered the decreased crystallite index. The difference in crystallinity of M1, M2 and M3 could be safely attributed to potential of the chlorite salts. For example, the M2 suggested that a use of 0.7 % acidic sodium chlorite over acidic sodium hypochlorite in M3 was adverse to obtain high crystallinity but resolute to maintain the cellulose structure.

The crystallinity index (CI) values of the cellulose extracted through the different methods were determined using the peak height method, in which the CI is calculated from the height of the 200 peak (I_{200}) and the height of the minimum between the 100 peak and the 200 peak (I_{AM}) using equation 3.1:

$$CI = \frac{I200 - I100}{I200} * 100 \quad \text{.....(3.1.)}$$

The *d*-spacing (d_{200}) was determined from the 2θ position of the d_{200} diffraction peak using Bragg's law:

$$n\lambda = 2d\sin\theta \quad \text{(3.2.)}$$

where n = 1 and λ= 1.542 Å; n is a positive integer and λ is the wavelength of the incident wave.

Table 2: Crystallinity index of the cellulose extracted through the different methods.

Method	*2θ (Main reflection)*	d_{200} *(nm)*	*Crystallinity index (%)*
1	23.08	0.39	68
2	22.98	0.39	73
3	22.63	0.39	67
4	23.32	0.38	72
5	22.63	0.39	70

3.3.5. TGA

Figure 3.8 represents TG and DTG curves of cellulose extracted from the different methods. All curves appear to follow a similar degradation mechanism with three degradation steps, in which the second step shoulders the third, except M1 which indicates a resolution of the second and third steps at approximately 250 and 300 ºC, respectively. In addition, M1 indicates the poorest thermal stability with highest char content, while M5 and M3 reveal higher thermal stability trailed by M4 and M2 respectively. These results seem to contradict the SEM results which suggested a better surface area for M1, but FTIR and XRD suggested the formation of cellulose derivatives. It is known in literature that lignin is catalytic to thermal degradation of celluloses,[13, 16] but in this case the derivatives seemed to dominate because all samples indicated the presence of lignin from the FTIR. Another factor may be the lining content or the nature of cellulose derivative which could explain the higher thermal stabilities of the other methods.

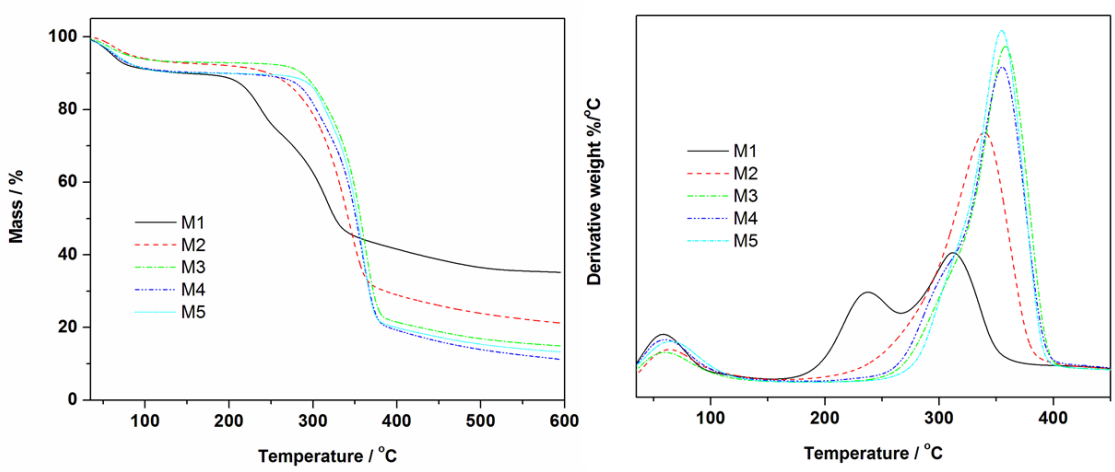

Figure 3.8: TG and DTG curves of the cellulose obtained from bagasse through the five extraction methods.

3.4. Conclusion

Cellulose has been successfully extracted from sugarcane bagasse through five different methods. The use of acidified sodium chlorite proved to be very effective in the digestion of SCB cell walls in contrast to the use of sodium hypochlorite. Acidified sodium hypochlorite yielded better results than its non-acidified counterpart. Characterization techniques showed cellulose extracted through the fifth method to have better properties trailed by method 4. The properties of the extracted materials are ideal for application as fillers in polymeric composites.

3.5. References

1. J.I. Moran, Alvarez, V.A., Cyras V.P., Vazquez A., *Cellulose* , 15, 2008, 149-159.
2. A. Mandal, D. Chakrabarty, *Carb. Polym.*, 86, 2011, 1291-1299.
3. H. Althues, J. Henle, S. Kaskel, *Chem. Soc. Rev.*, 36, 2007, 1454-1465.
4. V. Landry, A. Alemdar, P. Blachet, *Forest prod. J.*, 61, 2011, 104-112.
5. Kagarzadeh, I. Ahmad, I. Abdullah, A. Dufresne, S.Y. Zainudin, R.M. Sheltami, *Cellulose*, 19, 2012, 855-866.
6. S. S. Ray, M. Okamoto, *Prog. Polym. Sci.*, 28, 2003, 1539-1641.
7. Y. Habibi, L.A. Luca, O.J. Rojas, *Chem. Rev.*, 110, 2010, 3479-3500.
8. M.S. Peresin, Y. Habibi, A. Vesterinen, O.J. Rojas, J.J. Pawlak, J.V. Seppala, *Biomacromol.*, 11, 2010, 2471-2477.
9. S.M.L. Rosa, N. Rehman, M.I.G. de Miranda, S.M.B. Nachtigall. C.I.D. Bica, *Carb. Polym.* 87, 2012, 1131-1138.
10. A. Mandal, D. Chakrabarty, *Carb. Polym.*, 86, 2011, 1291-1299.
11. A. Kumar, Y. Singh Negi, V. Chadhary, N. Kant Bhardwaj. *J. Mater. Phys. and Chem.* 2, 2014, 1-8.
12. R. Liu, H. Yu, Y. Huang, *Cellulose*, 12, 2005, 25-34.
13. A. Alemdar, M. Sain, *Biores. Technol.*, 99, 2008, 1664-1671.
14. Y.M. Zhou, S.Y. Fu, L.M. Zheng, H.Y. Zhan, *eXpressPolym. Lett.*, 6, 2012, 794-804.
15. G. Han, S. Huan, J. Han, Z. Zhang, Q. Wu, *Mater.*, 17, 2014, 16-29.
16. M. Cherian, A.L. Leao, S.F. de Souza, S. Thomas, L.A. Pothan, M. Kottaisamy, *Carb. Polym.*, 81, 2010, 720-725.
17. H. Kagarzadeh, I. Ahmad, I. Abdullah, A. Dufresne, S.Y. Zainudin, R.M. Sheltami, *Cellulose*, 19, 2012, 855-866.
18. M. Mariano, N. El Kissi, A. Dufresne, *J. Polym. Sci. Part B: Polym. Phys.*, 00, 2014, 000-000.
19. J.I. Moran, Alvarez, V.A., Cyras V.P., Vazquez A., *Cellulose*, 15, 2008, 149-159.
20. A.G. Norman, S.H. Jenkins, *Biochem. J.*, 27, 1993, 818-831.
21. L.Y. Mwaikambo, M.P. Ansell, *J. Appl. Polym. Sci.*, 84, 2002, 2222-2234.

CHAPTER FOUR:

SYNTHESIS OF CNCs FROM CELLULOSE, THEIR CHARACTERIZATION AND THEIR APPLICATION IN THE SYNTHESIS OF CNC/Ag NANOCOMPOSITES

4.1. Introduction

The past few years have seen intense interest and research on nanotechnology, which is a modern branch of technology that deals with the synthesis and manipulation of the structure of particles ranging from 1 to 100 nm in size. The enhanced chemical, physical, and biological properties of nanoparticles which are based on their distribution, morphology and reduced size have seen them gain particular interest in a number of fields such as health care,[1,2] biomedical,[3] catalysis,[4] electronics,[5] food packaging,[6] mechanics,[7] drug delivery[8] and cosmetics,[9] to mention but a few.

The constant outbreak of infectious diseases resulting from different pathogenic bacteria, and the development of antibiotic resistance has motivated the critical search for new, more effective antibacterial and antimicrobial agents. With regards to this, silver nanoparticles have gained particular interest due to their superior antibacterial,[10] antifungal,[11] antiviral[12] and anti-inflammatory properties.[13] Silver nanoparticles can be used as wound dressings,[14] antiseptic sprays and fabrics,[15] topical creams,[16] in food packaging,[6] and in many other biomedical applications.[3] Silver has the ability to disturb enzymatic activities of microorganisms by disrupting their unicellular membranes,[17] hence its wide applicability as an antimicrobial agent.

The synthesis of metal nanoparticles, particularly silver nanoparticles, follows two general approaches; the top-down and the bottom-up approaches.[18, 19] The top-down approach usually involves the mechanical grinding of the bulk metals which is then followed by stabilization of the obtained nanosized metal particles through the addition of colloidal protecting agents. The bottom-up approach, in contrast, includes sonodecomposition, electrochemical methods and the reduction of metals, which is the most common method.

The top-down approach is quite expensive to facilitate. On the other hand, the bottom up approach usually involves the use of highly toxic organic and inorganic reducing agents such as sodium borohydride,[20] Tollen's reagent[21] and N-N-dimethyl formamide,[22] to mention a few. These toxic reducing agents lead to non-eco-friendly by-products, and may compromise the medicinal and antimicrobial properties of silver, hence diminishing its applicability.

Research and interest in silver nanoparticles is therefore slowly being structured towards the development of more environmentally-friendly synthetic methods.[23-26] This has led to the advancement of green synthetic methods over their physical and chemical counterparts. The

green synthetic methods are cost effective, environmentally friendly and are easily scaled up. They also avoid the use of high temperatures and pressures, and toxic chemicals.[27]

This chapter will focus on the use of cellulose nanocrystals (CNCs), which are a plant material, as a reducing and stabilizing agent in the formation of CNC/Au nanocomposites. The use of nontoxic plant materials is highly motivated since it does not diminish the antibacterial nature of silver nanoparticles.

4.2. Experimental

4.2.1. Materials

CNCs were prepared through acid hydrolysis from cellulose extracted from SCB (the cellulose extracted through the fifth method in Chapter 3 was used for this purpose). The SCB was obtained from Felixton sugar mill at Empangeni, South Africa. $AgNO_3$ and 98 % H_2SO_4 were purchased from Sigma Aldrich. H_2SO_4 was diluted to the desired concentration. Deionised water was used throughout the reactions.

4.2.1.1. Preparation of CNCs

CNCs were prepared through acid hydrolysis, which was conducted at 45 ºC under mechanical stirring using 60 wt% H_2SO_4. Basically, in a 250.0 mL beaker, 10.0 g cellulose was mixed with 150.0 mL H_2SO_4 preheated to 45 ºC. The mixture was constantly stirred for 30 minutes, after which the reaction was quenched with 10-fold excess cold distilled water. Stirring was continued for a further 5 minutes, after which the suspension was centrifuged at 4.4 rpm for 20 minutes. Centrifugation was repeated for three times, which was followed by ultrasonication. The resulting product was finally stored in the refrigerator.

4.2.1.2. Preparation of CNC/Ag nanocomposites

The CNC/Ag nanocomposites were prepared through hydrothermal synthesis. Basically, 0.5 g CNCs were dispersed in 10.0 mL distilled water. The dispersion was subsequently mixed with 10.0 mL $AgNO_3$ at different concentrations (50, 100 and 200 mM). Mixing was accomplished using a magnetic stirrer for 5 minutes. The respective mixtures were then transferred into Teflon-sealed glass bottles and heated at 110 ºC at different reaction times (8 and 24 hrs). The resulting mixtures were then centrifuged at 4.4 rpm for 10 minutes in order to remove unreacted salts. Centrifugation was repeated for three times, and the products were finally stored in a refrigerator.

4.2.2. Characterization

4.2.2.1. Fourier Transform Infrared (FTIR)

Infrared spectra of the samples were recorded on a Bruker FT-IR Tensor 27 spectrophotometer equipped with a standard ATR crystal cell detector. The spectra were recorded at a wavenumber range of 500-4000 cm^{-1}.

4.2.2.2. X- Ray Diffraction (XRD)

The diffraction patterns of the materials were investigated at room temperature using an Advanced Bruker AX D8 diffractometer in the range $2\theta = 14 – 90$ º, equipped with nickel-filtered Cu *Kα* radiation ($\lambda = 1.542$ Å) at 40 kV and 40 mA. The scan speed was 5 sec/step.

4.2.2.3. Scanning Electron Microscope (SEM)

The surface morphology of the nanocomposite materials was observed using a Zeiss EVO LS 15 ultra plus FESEM (scanning electron microscopy) fitted with oxford energy dispersive X-ray (EDX) detector. The CNC/Ag nanocomposites were coated with gold before analysis.

4.2.2.4. Ultraviolet-Visible (UV-Vis) spectroscopy

UV/Vis measurements were carried out on a Perkin Elmer Lambda 1050 UV/Vis/NIR spectrometer at a range of 350-700 cm^{-1}.

4.2.2.5. Transmission Electron Microscopy (TEM)

A JEOL 1400 TEM was used for analysis, at an accelerating voltage of 120 kV. A Megaview III camera was used and the images were captured using iTEM software. The samples were prepared by evaporating drops of diluted respective solutions on Formvar-coated Cu grids (150 mesh).

4.3. Results and discussion

For all the analytical techniques requiring dry samples, the samples were dried by centrifuging in a volatile solvent (acetone) followed by placing in a desiccator for five hours at moderate temperatures.

4.3.1. PART A: PREPARATION OF CNCs FROM CELLULOSE

4.3.1.1. FTIR

Figure 4.1 shows the FTIR spectra of cellulose and CNCs. The spectrum of CNCs greatly resembles that of cellulose. The broad bands in the region 3600-3000 cm^{-1} indicate the O-H stretching vibration of OH groups in cellulosic materials. At around 2883 cm^{-1} the spectra show characteristic C-H stretching vibrations. The spectra also show bands at 1365 cm^{-1}, which correspond to the bending vibration of the C-H and C-O bonds in the polysaccharide aromatic rings. The peaks observed at approximately 1643 cm^{-1} are due to the O-H bending of adsorbed water, and those at 1052 cm^{-1} can be attributed to the C-O-C pyranose ring stretching vibration.

Furthermore, the peaks at 1155 and 1105 cm^{-1} represent C-C breathing and C-O-C glycosidic ether bands, respectively. Both of these peaks arise from the polysaccharide components of cellulosic materials. In CNC, it can be noted that these peaks are gradually lost. This is a result of acid hydrolysis and a reduction in molecular weight.

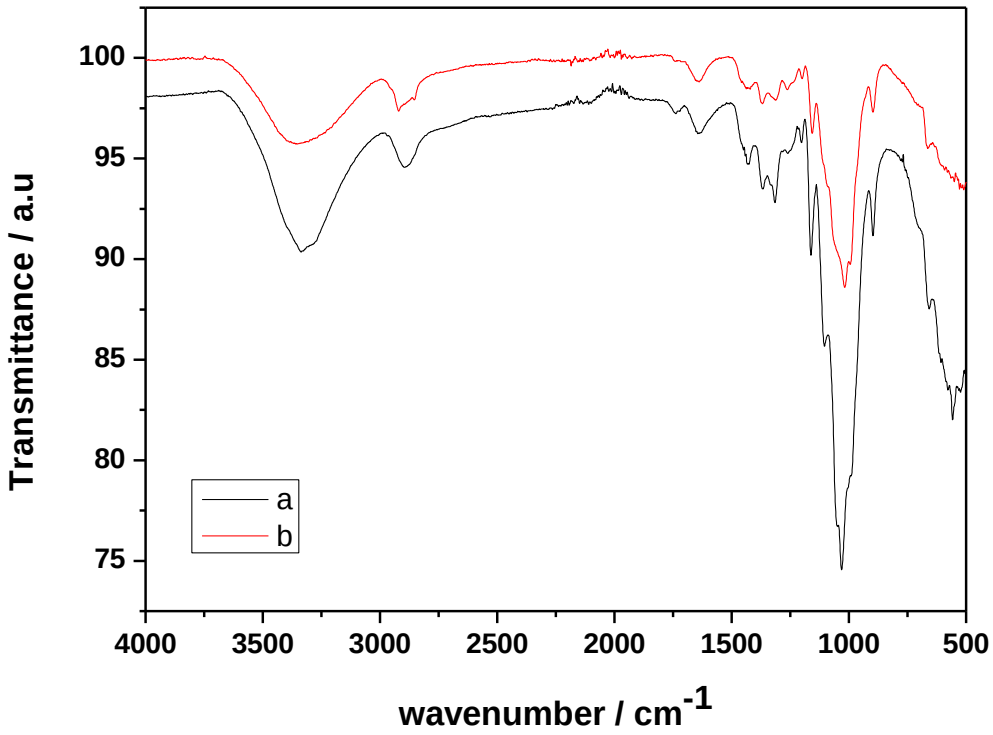

Figure 4.1: FTIR spectra showing a) cellulose, and b) CNCs

4.3.1.2. TEM

Figure 4.2 shows TEM micrographs of CNCs showing rod-like particles. Visible on the micrographs are individual nanocrystals and some aggregates. The appearance of aggregates can be attributed to the high specific area and the strong hydrogen bonds present in cellulose.

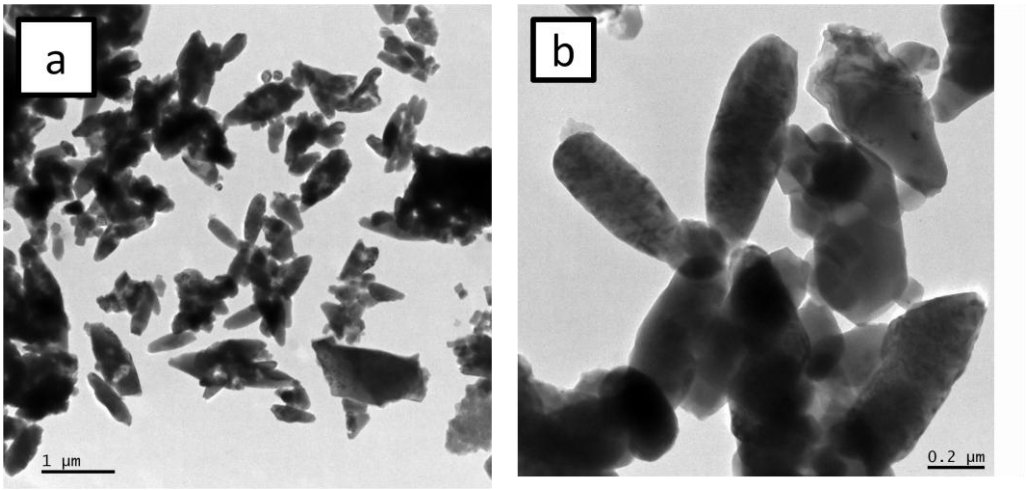

Figure 4.2: TEM micrographs of CNCs

4.3.1.3. XRD

Figure 4.3 shows the XRD patterns of cellulose and CNCs. The conditions under which CNCs were dried ended up not only reducing the amorphous portions, but also distorting the crystalline ones. A shift towards higher 2θ values is noted for CNCs (figure 2b), which can also be attributed to the drying method. All in all, the CNCs do show the two main peaks of cellulose, which are at 2θ values of 16.0 and 22.8 º, representative of 110 and 200 planes, respectively.

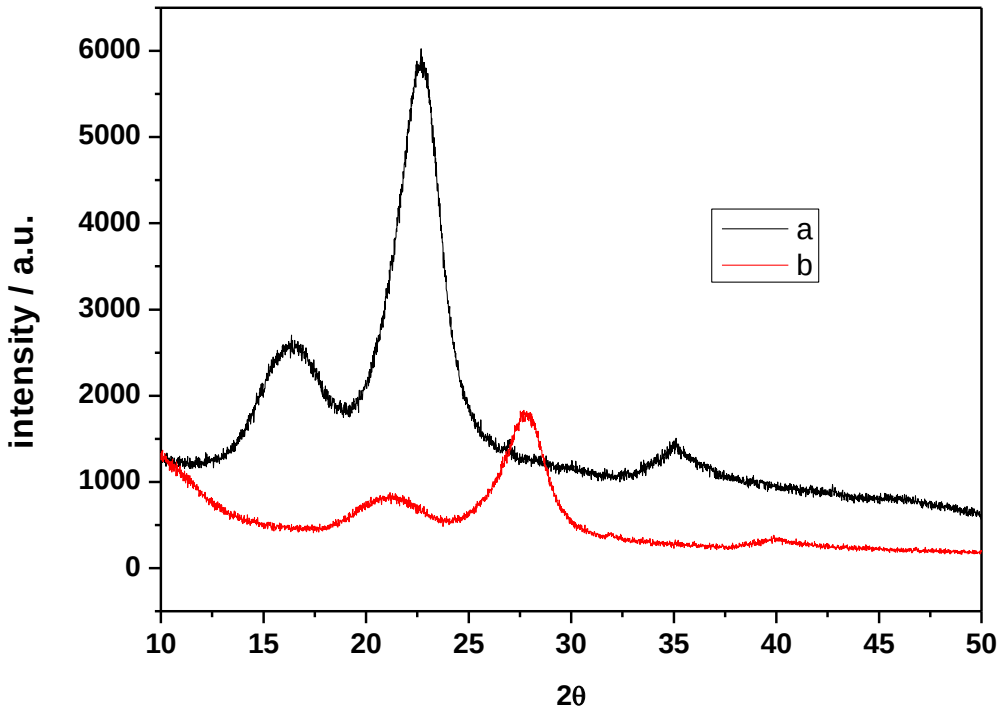

Figure 4.3: XRD patterns of a) cellulose, and b) CNCs

4.3.1.4. SEM

Figure 4.4 shows the SEM micrographs of cellulose (a) and cellulose nanocrystals (b). It was shown in Chapter 3 that sugarcane bagasse (SCB) fibres consist of many non-fibrous components that are scattered over their surface. The treatment of SCB with different chemicals resulted in the removal of the non-fibrous components and the subsequent thinning of the fibres.

The hydrolysis of cellulose with H_2SO_4 results in the removal of the amorphous regions, which results in further thinning of the fibres, as evident in Figure 4.4b. Furthermore, the surface of cellulose (Figure 4.4a) is slightly smoother in contrast to that of CNCs (Figure 4.4b). This may be attributed to the fact that acid hydrolysis results in a further removal of non-cellulosic components like oils and waxes that might have remained during the alkali treatment of SCB.

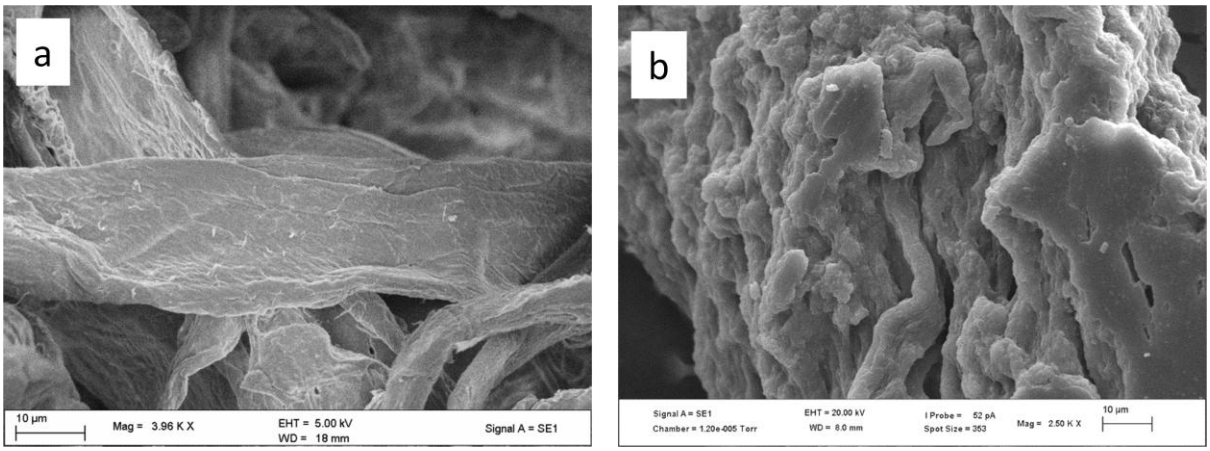

Figure 4.4: SEM micrographs of a) cellulose, and b) CNCs

4.3.2. PART B: SYNTHESIS OF CNC/Ag NANOCOMPOSITES

4.3.2.1. FTIR

Figures 4.4 and 4.5 show the FTIR spectra of the nanocomposite materials at 8 and 24 hours respectively. All the spectra show characteristic bands of CNCs, such as 3375 cm^{-1} (OH), 2915 cm^{-1} (CH_2), 1732 cm^{-1} (C=O), and 1163 cm^{-1} (C-O-C). This signifies the fact that Ag nanoparticles were able to attach on the pores of the CNCs, and that the CNCs were able to successfully stabilize the Ag nanoparticles and induce a small size distribution.

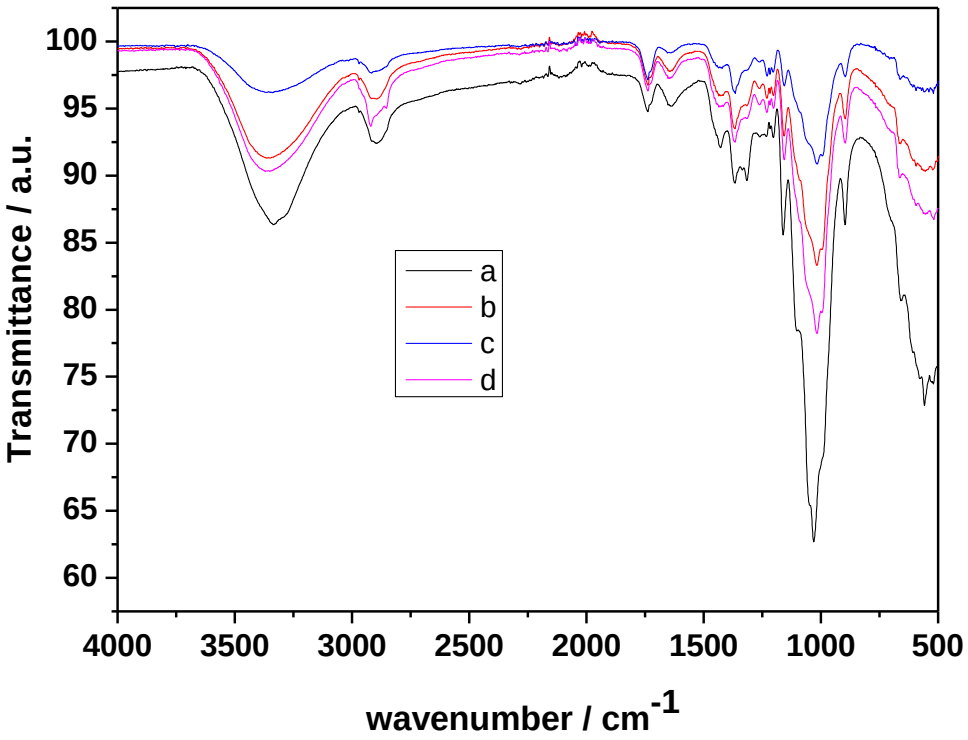

Figure 4.5: FTIR spectra showing (a) CNCs, and 8 hour reactions of CNC/Ag nanocomposites at (b) 50 mM, (c) 100 mM and (d) 200 mM concentrations

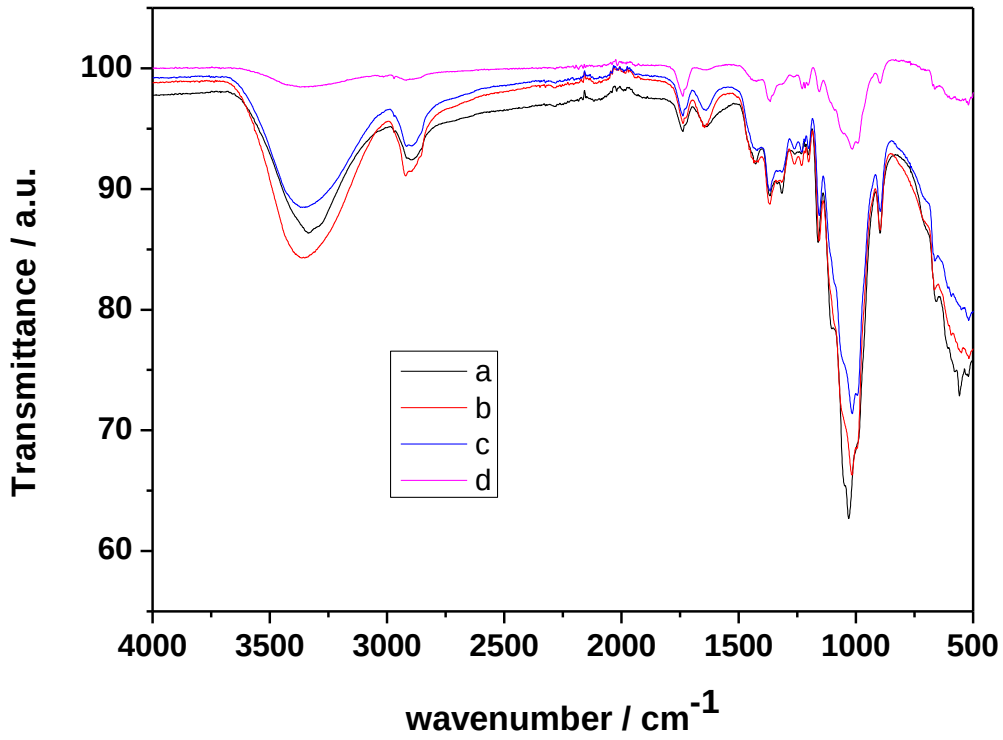

Figure 4.6: FTIR spectra showing (a) CNCs, and 24 hour reactions of CNC/Ag nanocomposites at (b) 50 mM, (c) 100 mM and (d) 200 mM concentrations.

4.3.2.2. TEM

Shown in Figure 4.6 are the TEM micrographs of the nanocomposite materials prepared at different concentrations and reaction times. The extensive hydroxyl groups on the cellulose nanocrystals act as anchoring sites for silver ions. The nanosized pores of the cellulose nanocrystals serve as the nanoreactor for the nucleation and growth of silver nanoparticles, restricting the growth of the particles within the pores, stabilizing the particles, and inducing a small size distribution. The addition of metals to polymers is expected to result in composites with improved properties and rigidity.

The population of the mostly-spherical CNC/Ag nanoparticles obtained increases with an increase in reaction time and silver concentration. It can also be noted that the size of the nanoparticles decrease with an increase in reaction time; that is, the particles obtained at 24 hrs are smaller relative to those obtained at 8 hrs for all the concentrations. The average nanoparticle sizes for the 8 hr reactions are 32.01 ± 21.13 nm, 11.46 ± 4.98 nm, and 24.51 ± 3.74 nm for 50, 100 and 200 mM $AgNO_3$ concentrations, respectively (Figure 3a, c and e). At

24 hrs a reduction in these sizes is seen, with 8.12 ± 2.84 nm, 7.04 ± 3.18 nm and 8.72 ± 3.69 nm average sizes obtained for the 50, 100 and 200 nm $AgNO_3$ concentrations, respectively (Figure 4.6b, d and f).

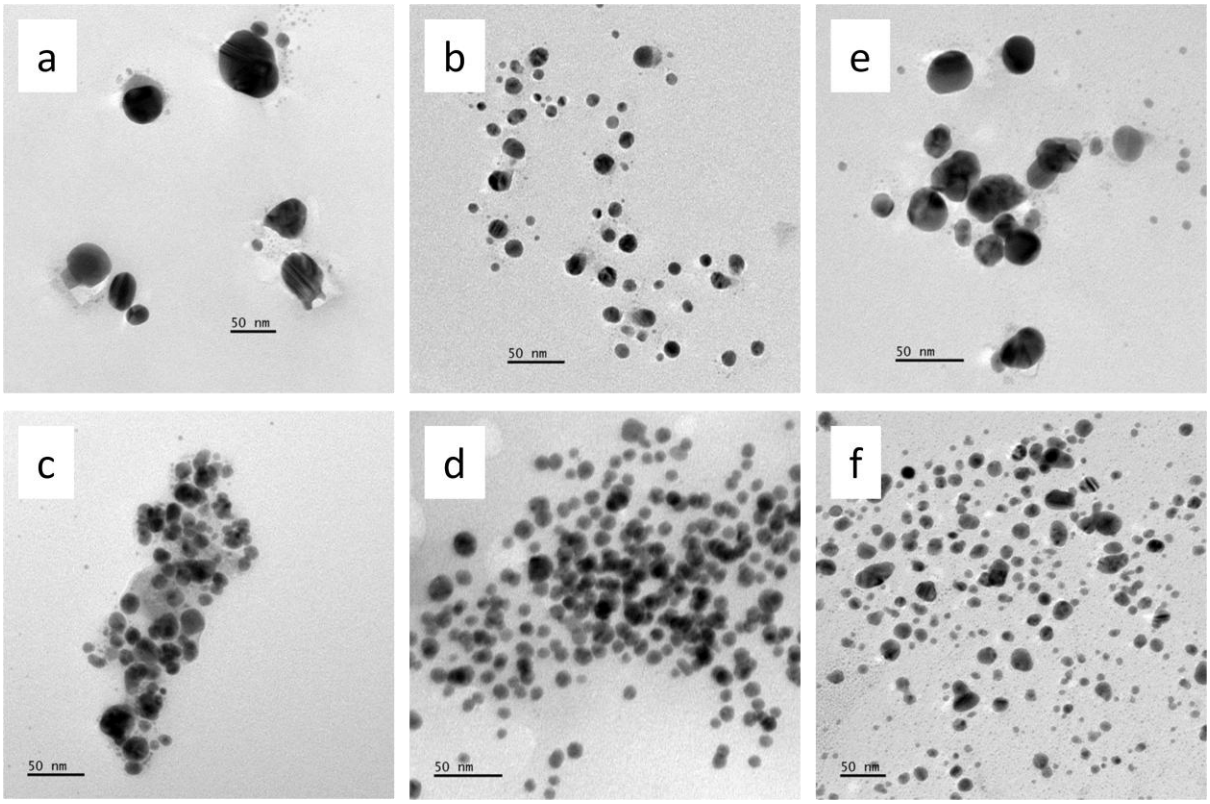

Figure 4.7: TEM micrographs of CNC/Ag nanocomposites at different reaction times and concentrations; 50 mM: (a) 8hrs, (b) 24 hrs; 100 mM: (c) 8 hrs, (d) 24 hrs and 200 mM: (e) 8 hrs, (f) 24 hrs.

4.3.2.3. UV-Vis

Figure 4.7 shows the UV- Visible spectra of CNC/Ag nanocomposites. The colour of the nanocomposites changed from light- to bright- and finally dark yellow with an increase in reaction time and $AgNO_3$ concentration. CNCs were used as the reference, and therefore the absorption spectra may be attributed to the absorption of Ag species. At all the concentrations and reaction times, the absorption band peaks are located at approximately 427 nm, and they can be attributed to the Surface Plasmon Resonance (SPR) of silver nanoparticles, which is in agreement with the yellow colours observed.[62] At wavelengths longer than 500 nm no absorptions were observed, which implies the formation of Ag nanoparticles with narrow size distributions.

It can also be noted that the absorption intensities of the Plasmon bands increase with an increase in reaction times and $AgNO_3$ concentrations. This is concurrent with the change of colour from light- to dark yellow. These factors can be attributed to the increase of silver loading.

At lower reaction times (8 hrs), relatively broader surface plasmons are observed, which suggests the formation of larger nanoparticles. As the reaction times are increased the surface plasmons narrow, implying the formation of smaller nanoparticles.

The UV/Vis results are in agreement with those of TEM in the sense that CNCs were successfully utilized as a stabilizing agent for the formation of Ag nanoparticles. They were also able to prevent the nanoparticles from aggregating.

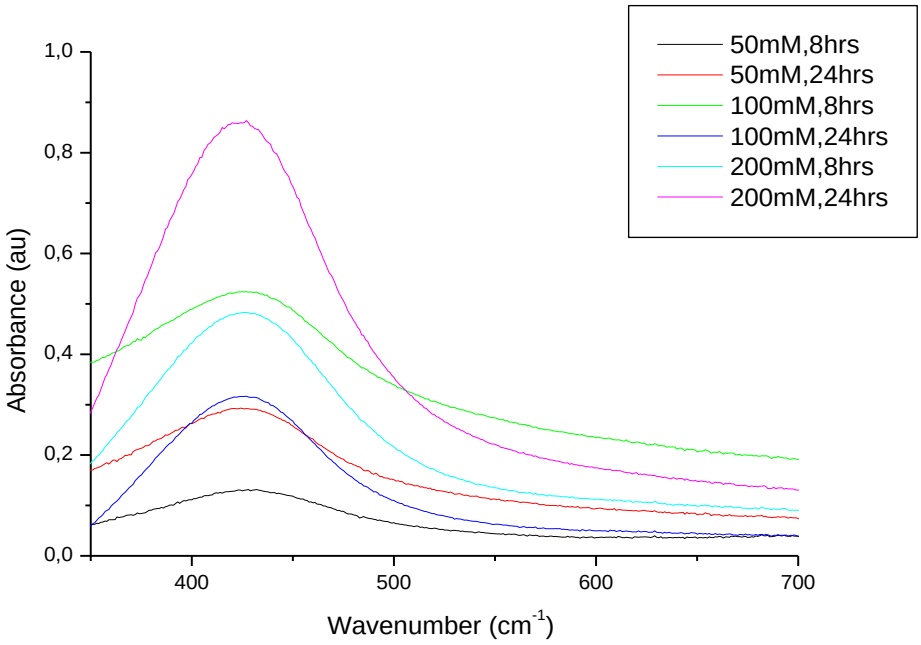

Figure 4.8: UV/Vis spectra of CNC/Ag nanocomposites at different reaction times and concentrations at 110 ºC.

4.3.2.4. XRD

The XRD patterns for CNC/Ag nanocomposites are shown in Figures 4.9 and 4.10 for 8 and 24 hour reactions, respectively. All the patterns at different concentrations and reaction times show reflections from CNCs and Ag crystals, signifying the formation of the nanocomposite materials. At 2θ = 21.1º, a peak corresponding to 200 diffractions of CNCs is observed throughout the samples. Another peak observed throughout the samples is that at 2θ = 38.3º, which is representative of the (111) planes of silver nanoparticles. At the lowest reaction concentration (50 mM), at both reaction times (8 and 24 hrs), some additional peaks representing the oxides of silver are observed. Those are at 2θ = 27.7, 32.7 and 46.8 º, which are representative of the (400), (110) and (132) diffraction planes of Ag_2O_3, Ag_2O and Ag_3O_4, respectively. An increase in reaction concentration is seen to result in the diminishing of the peaks at 2θ = 27.7, 32.7 and 46.8 º, giving more prominence to the peak at 2θ = 38.3º. The presence of the oxides may be attributed to the fact that CNC's are highly populated with OH groups.

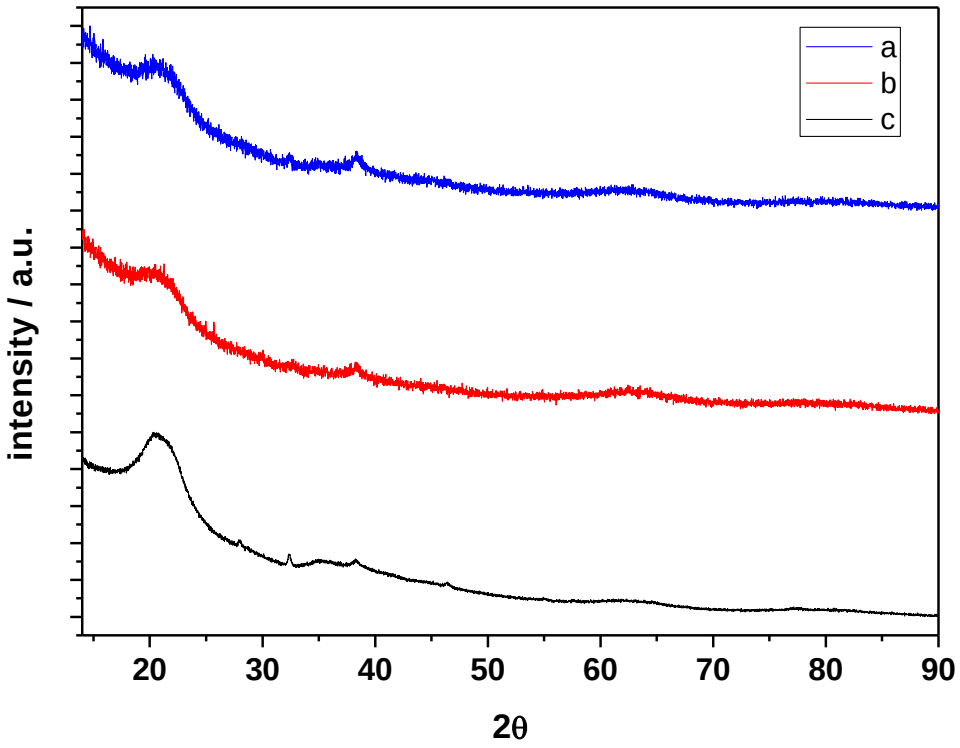

Figure 4.9: XRD patterns of CNC/Ag nanocomposites at 8 hrs, (a) 200 mM, (b) 100 mM and (c) 50mM.

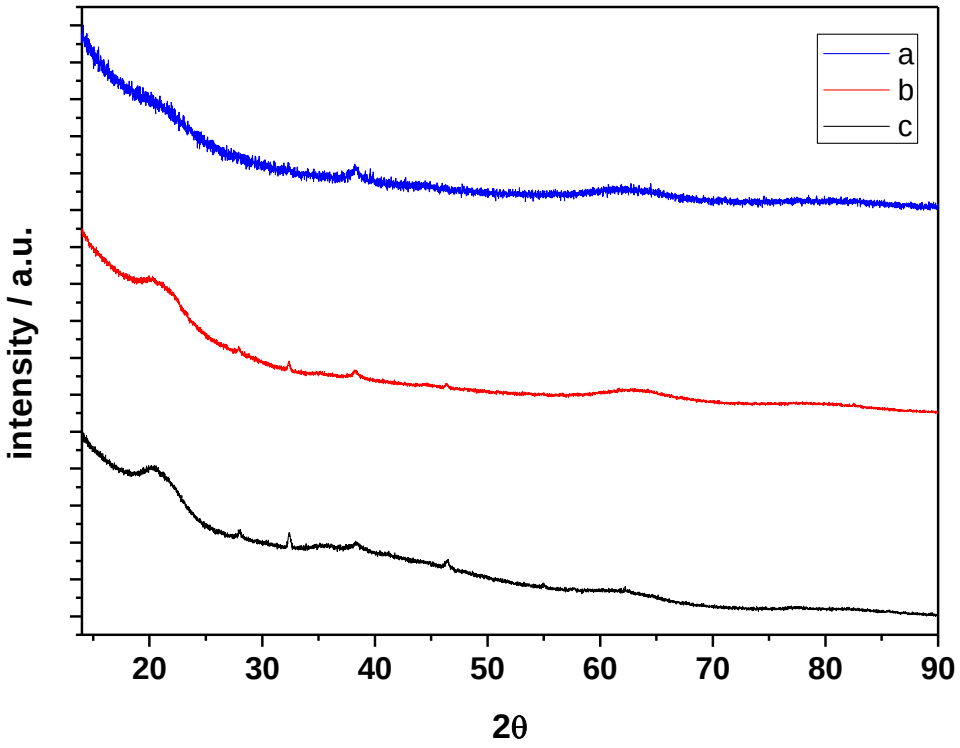

Figure 4.10: XRD patterns of CNC/Ag nanocomposites at 24 hrs, (a) 200 mM, (b) 100 mM and (c) 50mM.

4.3.2.5. SEM

Figure 4.11 shows the SEM micrographs of CNC/Ag nanocomposites synthesized at different reaction times and concentrations. The surfaces of all the CNC/Ag nanocomposites are slightly rougher in comparison to those of CNCs (Figure 4.4b), which can be attributed to the attachment of silver nanoparticles. TEM analysis of the nanocomposite materials (Figure 4.7) showed the formation of very small particles. These particles are therefore not clearly visible on the SEM micrographs, and their presence can be deduced from the appearance of relatively rougher surfaces.

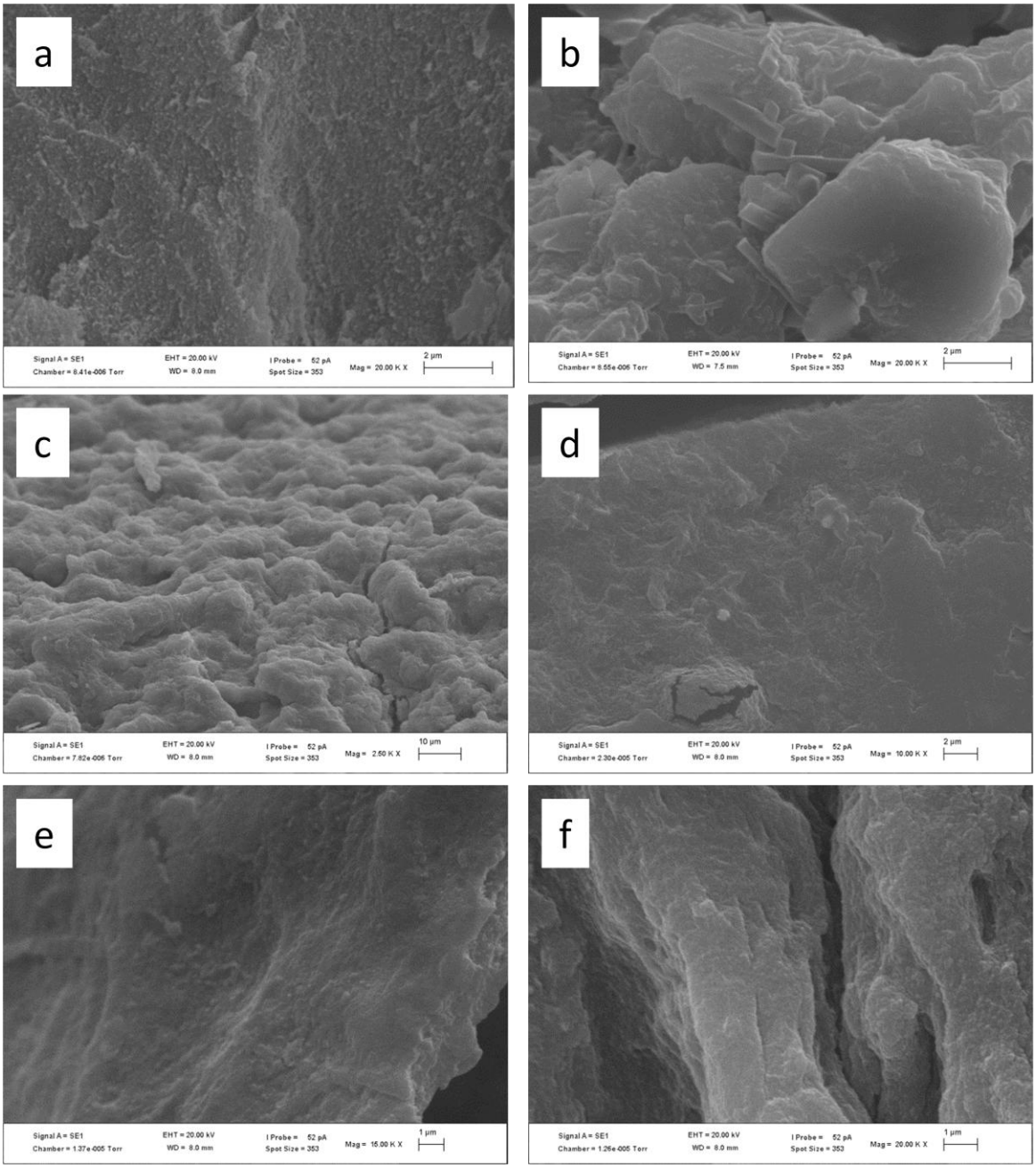

Figure 4.11: SEM micrographs of CNC/Ag nanocomposites at different reaction times and concentrations at 110 ºC; 1 mM: (a) 8hrs, (b) 24 hrs; 5 mM: (c) 8 hrs, (d) 24 hrs and 10 mM: (e) 8 hrs, (f) 24 hrs.

4.4. Conclusion

In this chapter, CNCs were successfully extracted from SCB and used as both a stabilizing and reducing agent in the formation of CNC/Ag nanocomposites. FTIR results of the nanocomposites showed that the structure of CNCs was preserved throughout the reactions, which implies that Ag nanoparticles were able to form and stabilize on the surface of CNCs with success. TEM micrographs and UV-Vis spectra were in agreement in that they both suggested and showed the formation of nanoparticles with narrow size distributions.

4.5. References

1. W.H. De Jong, P.J.A. Borm, *Int. J. Nanomed.*, 2008, 3(2), 133-149.
2. S.K. Sahoo, S. Parveen, J.J. Panda, *Nanomedicine: Nanotech., Bio. & Med.,* 2007, 3(1), 20-31.
3. P.G. Telegeeva, D.S. Iefremenko, G.D. Telegeev, S.S. Maliuta, *Biotechnol. Acta*, 2013, 6(2), 21-32.
4. M.C. Daniel, D. Astruc, *Chem. Rev.* 2004, 104(1), 293-346.
5. K. Balantrapa, D.V. Goia, *Mater. Res. Soc.*, 2009, 24(9), 2828-2836.
6. H.M.C. de Azeredo, *Food Res. Int.*, 2009, 42(9), 1240-1253.
7. K. Buyukhatipoglu, A.M. Clyne, *J. Biomed. Mater. Res.*, 2011, 96A(1), 186-195.
8. I.I. Slowing, B.G. Trewyn, S. Giri, V.S.Y. Lin, *Adv. Funct. Mater.,* 2007, 17(8), 1225-1236.
9. S.A. Wissing, R.H. Muller, *Int. J. Pharma.*, 2003, 254(1), 65-68.
10. I. Sondi, B. Salopek-Sondi, *J. Coll. and Int. Sci.*, 2004, 275(1), 177-182.
11. K.J. Kim, W.S. Sung, B. K. Suh, S.K. Moon, J.S. Choi, J.G. Kim, D. G. Lee, *Biometals*, 2009, 22(2), 235-242.
12. S. Galdiero, A. Falanga, M. Vitiello, M. Cintisani, V. Marra, M. Galdiero, *Molecules*, 2011, 16(10), 8894-8918.
13. P.L. Nadworny, J. Wang, E.E. Tredget, R.E. Burrel, *Nanomedicine: Nanotech. Biol. and Med.*, 2008, 4(3), 241-251.
14. T. Maneerung, S. Tokura, R. Rujiravanit, *Carb. Polym.*, 2008, 72(1), 43-51.
15. G. Zhang, Y.L.X. Gao, Y. Chen, *Nano. Res. Lett.*, 2014, 216(9), 1-8.
16. J. Jain, S.M. Rajwade, P. Omray, S. Khandlwal, K.M. Paknikar, *Mol. Pharma.*, 2009, 6(5), 1388-1401.
17. V.K. Sharma, R.A. Yngard, Y. Lin, *Adv. in Coll. and Interf. Sci.*, 2009, 145(1-2), 83-96.
18. D.K. Tiwari, J. Behari, P. Sen, *Curr. Sci.*, 2008, 95(5), 647-655.
19. Y. Wang, Y. Xia, *Nano. Lett.*, 2004, 4(10), 2047-2050.
20. L. Qi1, J. Ma, J. Shen, *J. Coll. and Interf. Sci.*, 1997, 186(2), 498-500.
21. M. Montazer, F. Alimohammadi, A. Shamei, M.K. Rahimi, *Carb. Polym.*, 2012, 87(2), 1706-1712.
22. I. Postoriza-Santos, L.M. Liz-Marzan, *Nano. Lett.*, 2002, 2(8), 903-905.
23. P. Raveendran, J. Fu, S.L. Wallen, *J. Am. Chem. Soc.*, 2003, 125, 13940-13941.

24. S. Iravani, *Green Chem.*, 2011, 13, 2638-2650.
25. H. Bar, D. Kr.Bhui, G.P. Sahoo, P. Sakar, S.P. De, A. Misra, *Coll. and Interf. A: Physiochem. & Eng. Asp.*, 2009, 339, 134-139.
26. M.N. Nadagouda, R.S. Varma, *Green Chem.*, 2008(10), 859-862.
27. J. Virkuyte, R.S. Varma, *Chem. Sci.*, 2011, 2, 837-846.

CHAPTER FIVE:

SYNTHESIS AND CHARACTERIZATION OF CNC/Au NANOCOMPOSITES

5.1. Introduction

Gold was, for a very long time, seen as merely a beautiful glittering metal. It was therefore used as an attractive ornamental piece of art and also as monetary coins.[1-3] As a result, it was generally seen as a symbol of wealth and power.

Gold has a much lower chemisorption power in contrast to platinum group metals.[4,5] The relatively low chemisorption ability of gold was believed to implicate a low catalytic power.[6] Scientific research into gold started taking shape when scientists realized that gold becomes really active when incorporated into supports as nanoparticles.[7,8] Like many other metal nanoparticles, gold nanoparticles have attracted a lot of attention due to their appealing electrical,[9] optical,[10] chemical[11] and catalytic properties[12] that are mostly dependant on their sizes and shapes.

Gold nanoparticles offer facile synthesis, good biocompatibility and conjugation to a number of biomolecular ligands and antibodies.[13-15] These properties make gold nanoparticles very suitable for use in medical diagnostics,[16] biomedical sensing and imaging,[17] and in therapeutic applications.[18] Gold has also found application in catalysis.[19] It has been reported that small supported gold nanoparticles can be utilized for the oxidation of CO at low temperatures.[20]

In this context, a lot of research has in the past few years been attributed to the synthesis of gold nanoparticles with controlled sizes and monodispersity.[21-24] Chemical methods are the mostly used in the synthesis of gold nanoparticles.[25-26] Of the many chemical methods, gold nanoparticles are generally prepared by reducing gold salts in the presence of a stabilizing agent, the function of which is to prevent the agglomeration of the particles.[27] The reducing and stabilizing agents may, however, remain unreacted in the solution, causing harm to the environment and also having adverse effects in biomedical applications.

Attention has, as a result been geared towards the development of synthetic methods that promote the use of rapid, cheap and reproducible approaches that have very minimal or no negative environmental effects. This attention is in line with the promotion, preservation and incorporation of the principles of green chemistry into the field of nanotechnology.

Gold, as a result of its applicability in a vast number of fields, has been a critical subject of green chemistry, green synthesis and subsequently, green nanotechnology. A lot of green

synthetic methods have been developed and used for the synthesis of gold nanoparticles. These synthetic methods aim to foster, amongst many things, the use of renewable feedstock, the use of benign solvents and auxiliaries, and the use of less hazardous synthetic methods.[28, 31]

Many plant materials have been used with great success for the synthesis of gold nanoparticles.[32-34] Very recently, polymeric materials have been the subject of critical studies for their use in the synthesis of gold nanoparticles.[35, 36]

In light of the aforementioned interest in the promotion of green synthetic methods, this chapter will focus on the use of cellulose nanocrystals (CNCs) as both a reducing and stabilizing agent in the formation of CNC/Au nanocomposites. The CNCs will be derived from an agricultural waste material (sugarcane bagasse), and the nanocomposite synthesis method will be water-based, hence its "green" nature.

5.2. Experimental

5.2.1. Materials

CNCs were prepared as in Chapter 4. $HAuCl_4$ was purchased from Sigma Aldrich. Distilled water was used throughout the reactions.

5.2.2. Preparation of CNC/Au nanocomposites

The CNC/Au nanocomposites were prepared through hydrothermal synthesis. 0.5 g CNCs were dispersed in 10.0 mL distilled water. The dispersion was subsequently mixed with 10.0 mL $HAuCl_4$ at different concentrations (1, 5 and 10 mM). Mixing was accomplished using a magnetic stirrer for 5 minutes. The respective mixtures were then transferred into Teflon-sealed glass bottles and heated at 110 ºC at different reaction times (8 and 24 hrs). The resulting mixtures were then centrifuged at 4.4 rpm for 10 minutes in order to remove unreacted salts. Centrifugation was repeated for three times, and the products were finally stored in a refrigerator.

5.2.3. Characterization

5.2.3.1. Fourier Transform Infrared (FTIR)

Infrared spectra of the samples were recorded on a Bruker FT-IR Tensor 27 spectrophotometer equipped with a standard ATR crystal cell detector. The spectra were recorded at a wavenumber range of 500-4000 cm^{-1}.

5.2.3.2. X- Ray Diffraction (XRD)

The diffraction patterns of the materials were investigated at room temperature using an Advanced Bruker AX D8 diffractometer in the range $2\theta = 14 – 90$ º, equipped with nickel-filtered Cu $K\alpha$ radiation ($\lambda = 1.542$ Å) at 40 kV and 40 mA. The scan speed was 5 sec/step.

5.2.3.3. Scanning Electron Microscope (SEM)

The surface morphology of the nanocomposite materials was observed using a Zeiss EVO LS 15 ultra plus FESEM (scanning electron microscopy) fitted with oxford energy dispersive X-ray (EDX) detector. The CNC/Au nanocomposites were coated with carbon before analysis.

5.2.3.4. Ultraviolet-Visible (UV-Vis) spectroscopy

UV/Vis measurements were carried out on a Perkin Elmer Lambda 1050 UV/Vis/NIR spectrometer at a range of 350-700 cm^{-1}.

5.2.3.5. Transmission Electron Microscopy (TEM)

A JEOL 1400 TEM was used for analysis, at an accelerating voltage of 120 kV. A Megaview III camera was used and the images were captured using iTEM software. The samples were prepared by evaporating drops of diluted respective solutions on Formvar-coated Cu grids (150 mesh).

5.3. Results and discussion

For all the analytical techniques requiring dry samples, the samples were dried by centrifuging in a volatile solvent (acetone) followed by placing in a desiccator for five hours at moderate temperatures.

5.3.1. TEM

Figure 5.1 shows the TEM images of the CNC/Au nanocomposites at different reaction times and concentrations at 110 ºC. Table 5.1 shows a summary of the sizes obtained. The TEM images for the 1 mM reactions show a mixture of triangular and spherical shapes for both reaction times (8 and 24 hrs, Figure 1 a and b, respectively). The spheres are dominant in both cases. At 8 hrs, the average size of the nanoparticles was found to be 19.73 ± 8.81 nm, whereas at 24 hrs it was found to be 13.85 ± 5.51 nm. At 5 mM concentrations, very big particles were obtained for both reaction times (8 and 24 hrs, Figure 5.1 c and d, respectively). As the concentrations are further increased to 10 mM, spherical nanoparticles with average sizes of 5.96 ± 1.49 nm were obtained at 8 hrs. At 24 hrs, irregular-pentagon-shaped nanoparticles with average sizes of 225 ± 29.95 nm were obtained.

Concentration	Reaction time (hrs)	Average sizes (nm)	Standard deviation (nm)
1 mM	8	19.73	± 8.81
	24	13.85	± 5.51
10 mM	8	5.96	± 1.49
	24	225	± 29.95

Table 5.1: A summary of the nanoparticle sizes obtained through TEM analysis.

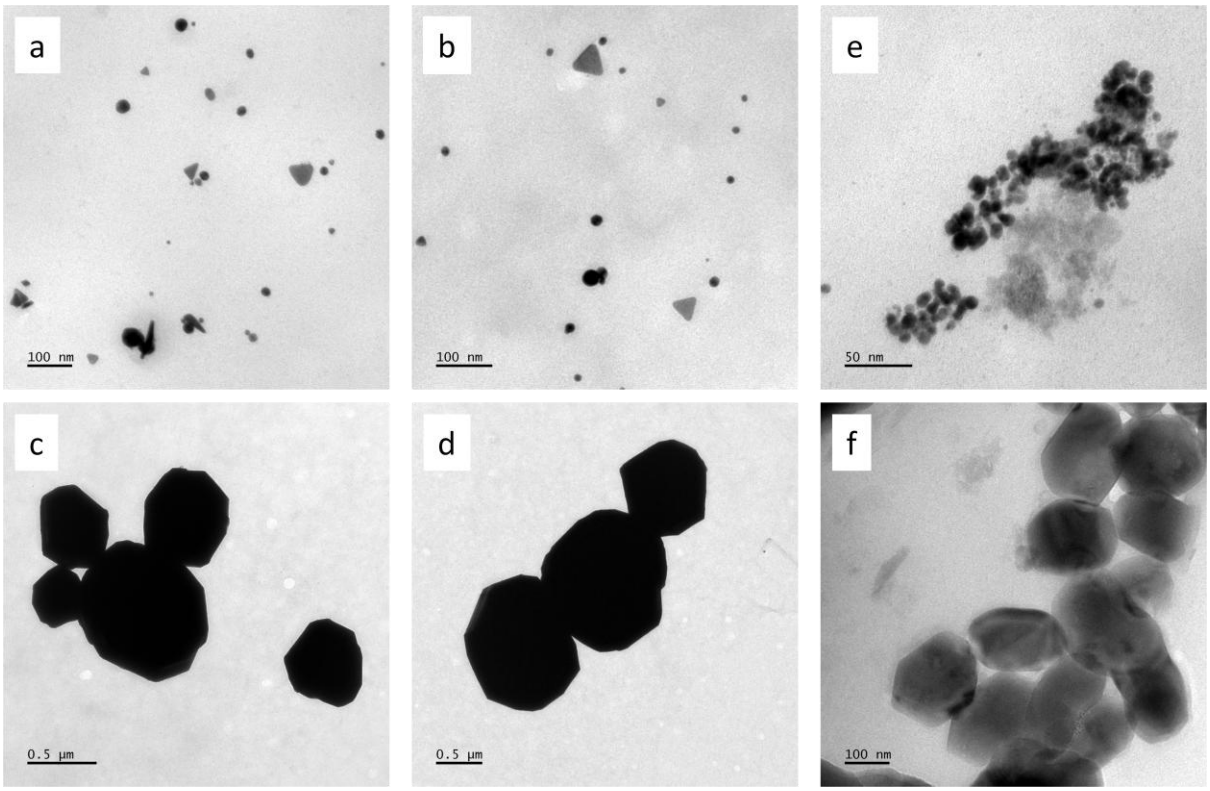

Figure 5.1: TEM micrographs of CNC/Au nanocomposites at different reaction times and concentrations at 110 ºC; 1 mM: (a) 8hrs, (b) 24 hrs; 5 mM: (c) 8 hrs, (d) 24 hrs and 10 mM: (e) 8 hrs, (f) 24 hrs

5.3.2. UV-Vis

Figures 5.2 and 5.3 show the UV-Vis spectra of the nanocomposite samples synthesized at 8 and 24 hrs, respectively. The reduction of $AuCl_4^-$ was visually evident from the change of colour from dark orange to ruby-red, which is an indication of the formation of gold

nanoparticles.[138] The UV-Vis spectra of the samples at both reaction times (8 and 24 hrs, Figures 5.2 and 5.3, respectively) show broad absorption bands between 487 and 536 nm, which are characteristic for gold nanoparticles. At 5 mM concentration no absorption was observed for the 8 hr reaction, and the plot for this reaction was therefore omitted. For the 24 hr reactions, the 5 mM spectrum shows a smaller band in contrast to the other concentrations (1 and 10 mM). These observations are in agreement with the formation of large particles at 5 mM concentrations as evident from TEM analysis.

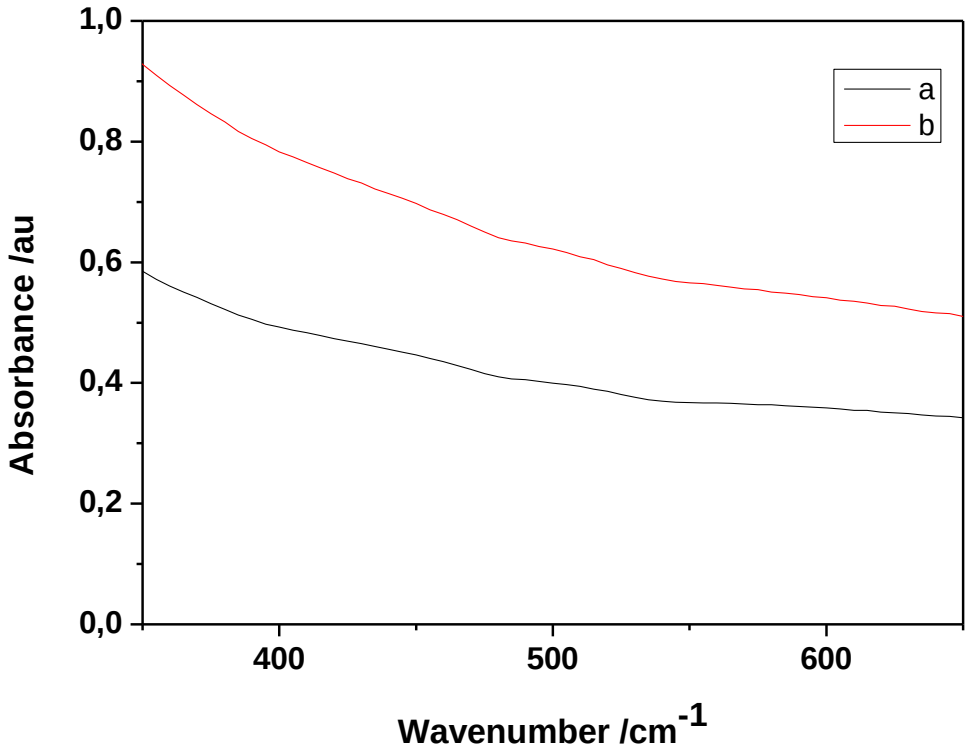

Figure 5.2: UV-Vis spectra showing CNC/Au nanocomposites synthesized at 110 ºC for 8 hrs at different concentrations: a) 1 mM and b) 10 mM.

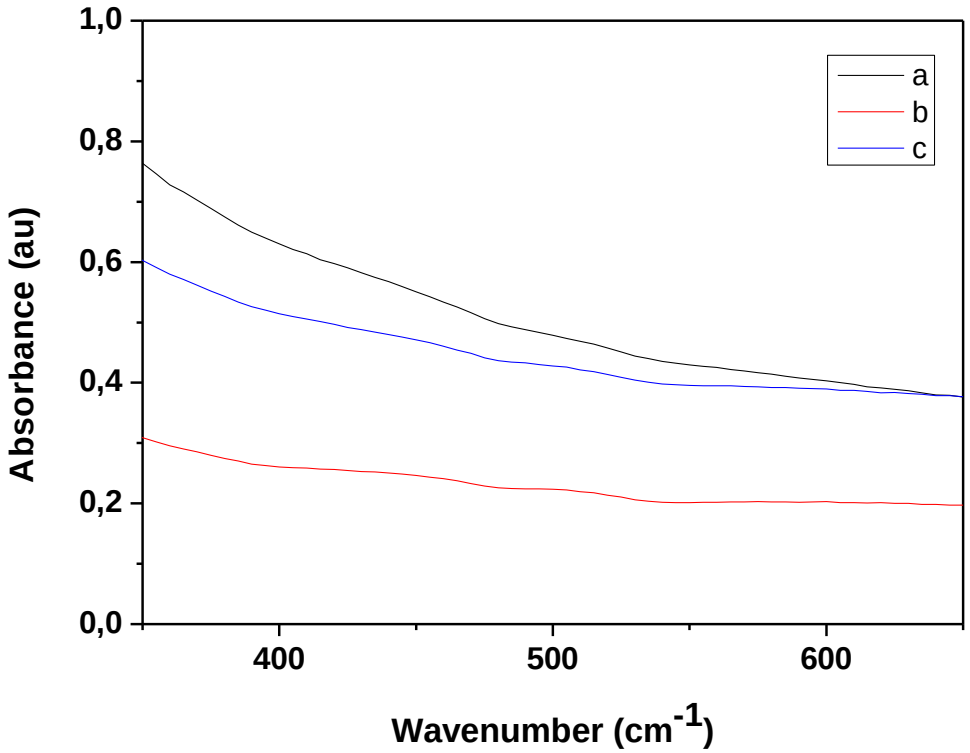

Figure 5.3: UV-Vis spectra showing CNC/Au nanocomposites synthesized at 110 ºC for 24 hrs at different concentrations: a) 1 mM, b) 5mM and c) 10 mM.

5.3.3. FTIR

The FTIR spectra of CNCs and CNC/Au nanocomposites synthesized at different reaction times and concentrations are shown in Figures 5.4 and 5.5. Figure 5.4 shows the 8 hr reactions, and Figure 5.5 shows the 24 hr reactions. All the spectra show characteristic bands of CNCs, such as 3375 cm^{-1} (OH), 2915 cm^{-1} (CH_2) and 1163 cm^{-1} (C-O-C). However, it can be observed that the band at 1732 cm^{-1}, representative of the carbonyl group (C=O) in CNC has shifted to lower wavenumbers (1643 cm^{-1}) for all the composite nanomaterials. This may suggest that gold binds through the carbonyl groups of CNCs during the formation of CNC/Au nanocomposites. This observation may be used to explain the catalytic nature of gold nanoparticles, as reviewed in chapter two of this thesis. It is known that metal carbonyls are highly applicable in organic synthesis and as catalyst precursors in homogeneous catalysis. [36]

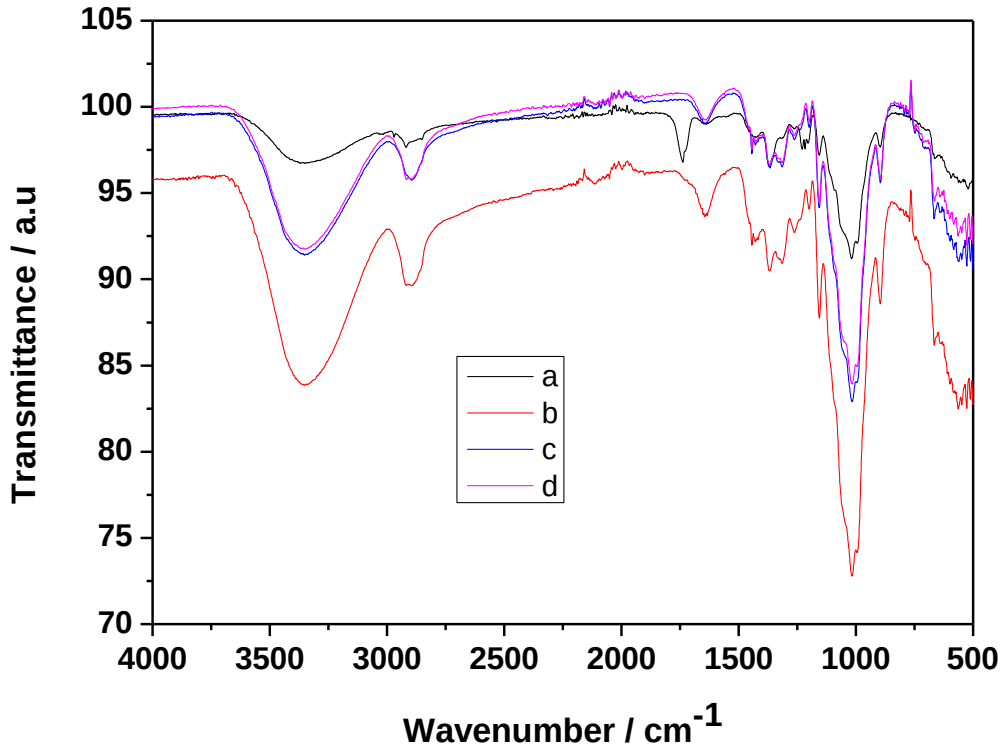

Figure 5.4: FTIR spectra showing (a) CNC, and 8 hour reactions of CNC/Au nanocomposites at (b) 1 mM, (c) 5 mM and (d) 10 mM concentrations.

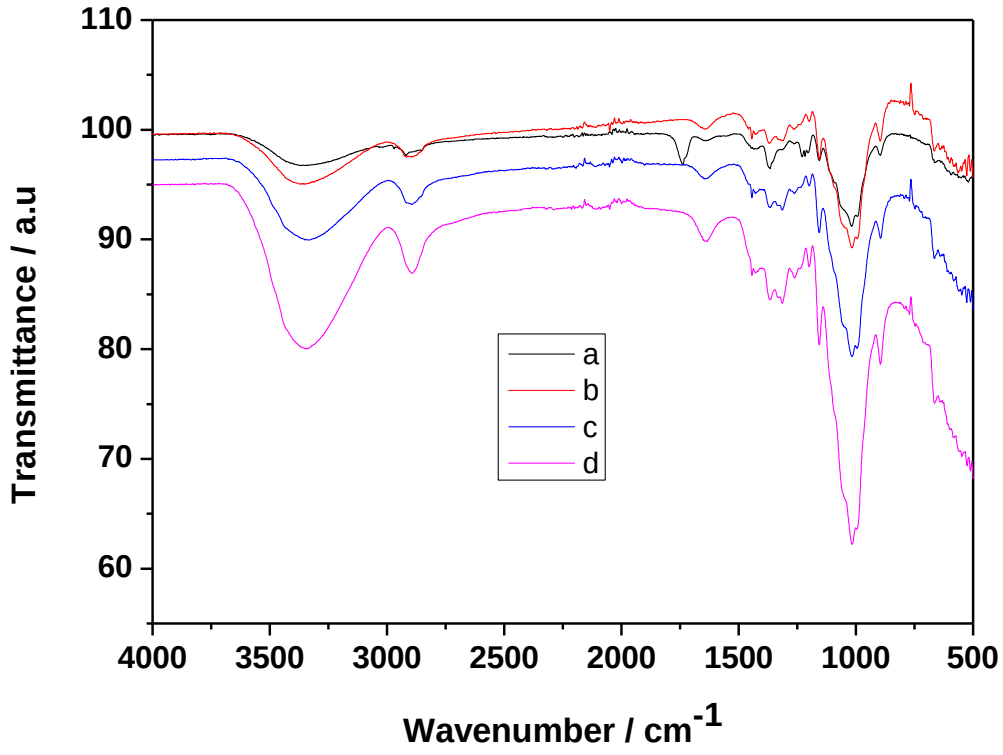

Figure 5.5: FTIR spectra showing (a) CNCs, and 24 hour reactions of CNC/Au nanocomposites at (b) 1 mM, (c) 5 mM and (d) 10 mM concentrations.

5.3.4. XRD

The XRD patterns for CNC/Au nanocomposites are shown in Figures 5.6 and 5.7 for 8 and 24 hour reactions, respectively. All the patterns at different concentrations and reaction times show reflections from CNCs and Au crystals, signifying the formation of the nanocomposite materials. At around 2θ = 21.0 º, a broad peak corresponding to the (200) diffractions of CNCs is observed throughout the samples. However, this peak decreases as the Au concentration is increased. This is true for both the 8 and 24 hr reactions (Figures 6 and 7, respectively). Furthermore, the XRD patterns show four peaks at 2θ = 38.2 º, 44.3 º, 64.7 º and 77.8 º in the 2θ range between 30 – 80 º. These peaks can be indexed to the (110), (200), (220) and (311) reflections of the fcc structure of metallic gold, respectively.

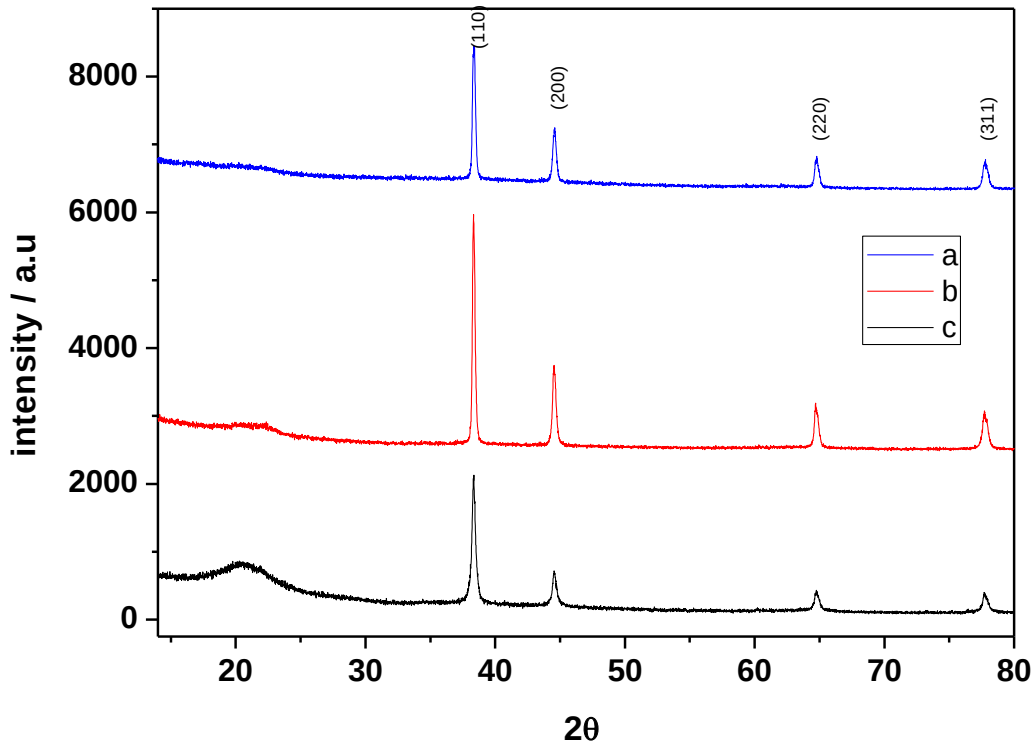

Figure 5.6: XRD patterns of CNC/Au nanocomposites at 8 hrs and (a) 10 mM, (b) 5 mM and (c) 1 mM concentrations.

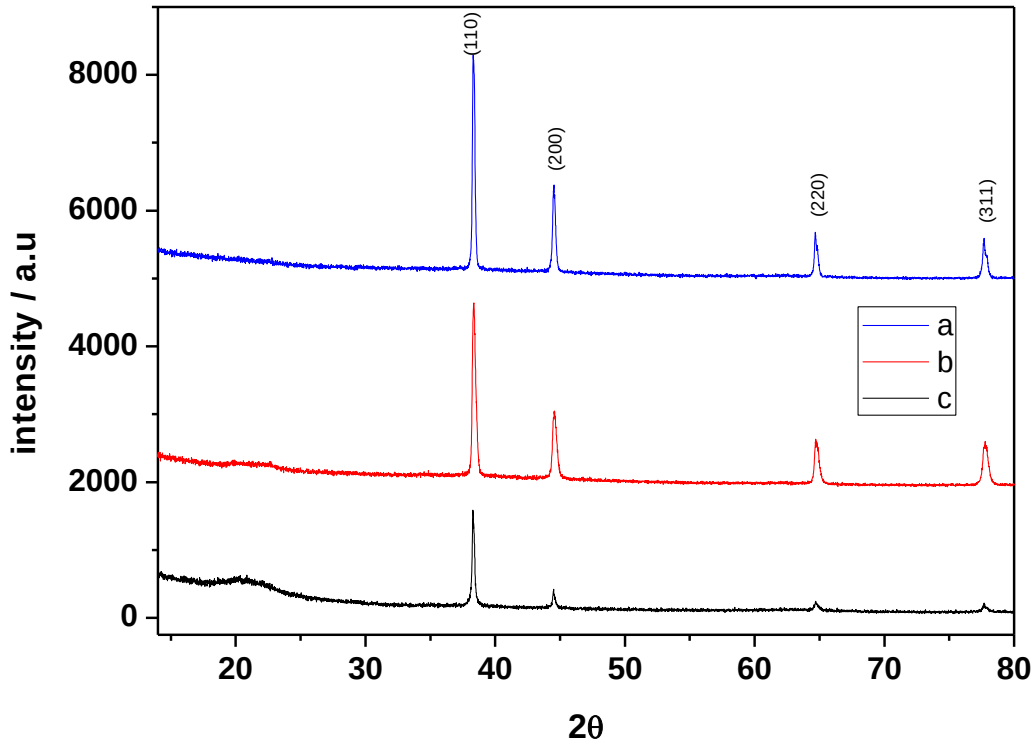

Figure 5.7: XRD patterns of CNC/Au nanocomposites at 24 hrs and (a) 10 mM, (b) 5 mM and (c) 1 mM concentrations.

5.3.5. SEM

Shown in Figure 5.8 are the SEM micrographs of CNC/Au nanocomposites synthesized at different reaction times and concentrations. The different reaction concentrations and times are seen to play vital roles in the deposition of gold nanoparticles onto the surface of CNCs. An increase in reaction concentration is seen to accelerate the deposition of gold nanoparticles on the surface of CNCs.

At all the reaction concentrations (1, 5 and 10 mM), the 24hr reactions result in the formation of clearly distinguishable, mostly-spherical shapes. On the other hand, the lower reaction times (8 hrs) result in the formation of clustered particles on the surfaces of the CNCs. This means that the reaction time is a crucial factor in the formation of the nanocomposite materials.

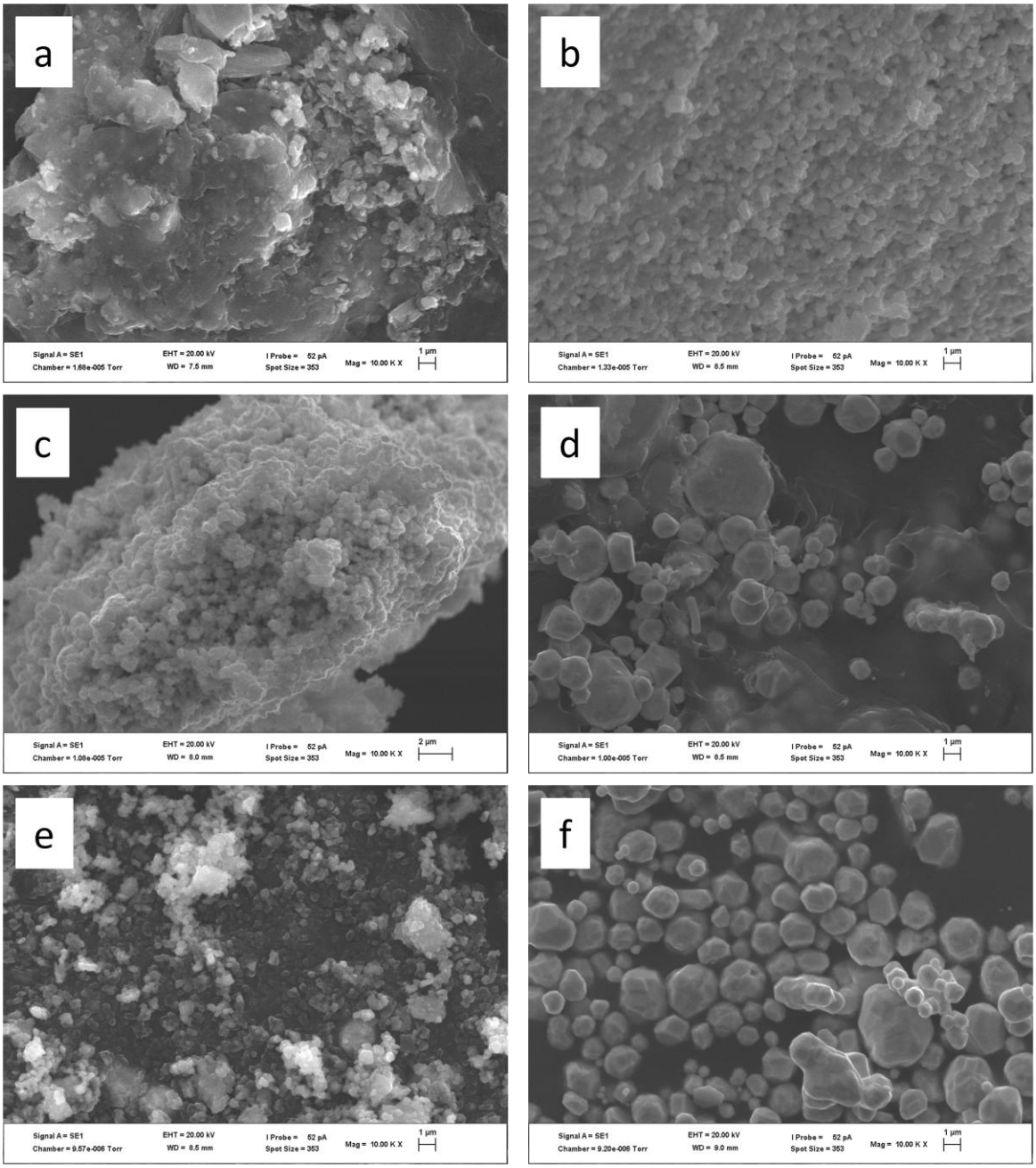

Figure 5.8: SEM images of CNC/Au nanocomposites at different reaction times and concentrations at 110 ºC; 1 mM: (a) 8hrs, (b) 24 hrs; 5 mM: (c) 8 hrs, (d) 24 hrs and 10 mM: (e) 8 hrs, (f) 24 hrs.

5.4. Conclusion

In this chapter, CNCs were successfully utilized as a reducing and stabilizing agent for the formation of CNC/Au nanocomposites. FTIR spectra of the samples suggest that gold binds through the carbonyl groups of CNCs during the formation of the nanocomposite materials, which renders the nanocomposites potentially applicable in catalysis. The XRD patterns show the formation of highly crystalline materials.

5.5. References

1. J. Evans, *Num. Chron. and J. Num. Soc.*, 12, 1850, 127-137.
2. A. Redish, *J. Econ. Hist.*, 4, 1990, 789-805.
3. M.E. Solt, P.J. Swanson, *J. Bus.*, 54, 3, 1981, 453-478.
4. P. Biloen, F.M. Dautzenberg, W.M.H. Sachtler, *J. Catalysts*, 50, 1977, 77-86.
5. G.C. Bond, *Gold Bulletin*, 34 (4), 2001, 117-119.
6. R. Zeis, A. Mathur, G. Fritz, J. Lee, J. Erlebacher, *J. Power Sourc.*,165 (1), 2007, 65-72.
7. S.E. Lohse, C.J. Murphy, *Chem. Mater.*, 25 (8), 2013, 1250-1261.
8. H.S. Zhou, I. Honma, H. Komiyana, *Phys. Rev. B*, 50 (16), 1994, 12052-12057.
9. G. Schmid, U. Simon, *Chem. Commun.*, 2005, 697-710.
10. C.L. Nehl, H. Liao, J.H. Hafiner, *Nano. Lett.*, 6 (4), 2006, 683-688.
11. D.A. Giljohann, D.S. Seferos, W.L. Daniel, M.D. Massich, P.C. Patel, C.A. Mirkin, *Angew. Chem. Int. Ed.*, 49, 2010, 3280-3294.
12. M.Valden, X. Liai, D.W. Goodman, *Science*, 281, 5383, 1998, 1647-1650.
13. E.C. Dreaden, A.M. Alkilany, X. Huang, C.J. Murphy, M.A. El-Sayed, *Chem. Soc. Rev.*, 41 (1), 2012, 2740-2779.
14. A. Schroedter, H. Weller, *Angew. Chemie*, 41(17), 2002, 3218-3221.
15. W. Eck, G. Craig, A. Sigdel, G. Ritters, R.J. Olds, L. Tang, M.F. Brennan, P.J. Allen, M.D. Mason, *ACS Nano.*, 2 (11), 2008, 2263-2272.
16. J.F. Hainfeld. D.N. Slatkin, T.M Focella, H.M. Smilowitz, *British J. Radiology*, 76 (1), 2006, 248-253.
17. K.S. Lee, M.A. El-Sayed, *J. Phys. Chem. B.*, 110 (39), 2006, 19220-19225.
18. D. Pissuwan, S.M. Valenzuela, M.B. Cortie, *Trends in Biotechnol.*, 24 (2), 2006, 62-67.
19. A. Abad, A. Corma, H. Garcia, *Chem. Eur J.*, 14 (1), 2008, 212-222.
20. M. Haruta, N. Yamada, T. Kabuyash, S. Lijima, *J. Catalysis*, 115 (2), 1989, 301-309.
21. Y. Sun, Y. Xia, *Science*, 298 (1),2002, 2176-2179.
22. I. Hussain, S. Graham, Z. Wang, B. Tan, D.C. Sherrington, S.P. Rannard, A.I. Cooper, M. Brust, *J. Am. Chem. Soc.*, 127 (47), 2005, 16398-16399.
23. N. R. Jana, L. Gearheart, C. J. Murphy, *Langmuir*, 17 (22), 2001, 6782-6786.
24. H. Hiramatsu, F.E. Osterloh, *Chem. Mater.*, 16 (13), 2004, 2509-2511.
25. S.D. Perrault, W.C.W. Chan, *J. Am. Chem. Soc.*, 131 (47), 2009, 17042-17043.

26. J. Kimling, M. Maier, B. Okenve, V. Kotaidis, H. Ballot, A. Plech, *J. Phys. Chem B,* 110 (32), 2006, 15700-15707.
27. S. Chen, K. Kimura, *Langmuir*, 15 (1), 1999, 1075-1082.
28. B. Nikoobakht, M.A. El-Sayed, *Chem. Mater.*, 15 (10), 2003, 1957-1962.
29. S.L. Smitha, D. Philip, K.G. Gopchandran, *Spectroch. Acta Part A*, 74 (1), 2009, 735-739.
30. H.R. Ghorbani, *Oriental J. Chem.*, 31 (1), 2015, 303-305.
31. S.A. Aromal, D. Philip, *Spectroch. Acta Part A*, 97 (1), 2012, 1-5.
32. J.Y. Song, B.S. Kim, *Bioprocess and Biosyst. Eng.*, 32 (79), 1-9.
33. D. Philip, *Spectroch. Acta Part A,* 77 (1), 2010, 807-810.
34. V.G. Kumar, S.D. Gokavarapa, A. Rajeswari, T.S Dhas, V. Karthick, Z. Kapadia, T. Shresta, I.A. Barathy, A. Roy, S. Sinha, *Coll. and Surf. B,* 87 (1), 159-163.
35. H. Huang, X. Yang, *Carb. Res.*, 339 (15), 2627-2631.
36. D.C. Bailey, S.H. Langer, *Chem. Rev.*, 81 (2), 1981, 109-148.

CHAPTER SIX:

CONCLUSIONS AND RECOMMENDATIONS

6.1. Summary and Conclusion

The work reported in this thesis is based on the extraction of cellulose from sugarcane bagasse (SCB), the synthesis of cellulose nanocrystals (CNCs) from the cellulose, and their subsequent application as a template, reducing- and stabilizing agent in the synthesis of silver and gold nanocomposites.

This research, and the synthetic methods employed herein were "green" in three major aspects. Firstly, cellulose was extracted from a waste material (SCB), thereby preventing waste; secondly, water was used as the only solvent in the synthesis of the nanocomposite materials, and therefore the syntheses of the nanocomposites were by all means not hazardous; and thirdly, the use of water as the only solvent ensured the use of safer solvents and/ or auxiliaries.

Cellulose was extracted from SCB through five different methods. According to the results, the fifth method yielded the most pure and thermally stable cellulose as depicted by the various analytical techniques employed. As a result, the cellulose extracted through this method was used to synthesize cellulose nanocrystals through acid hydrolysis. The nanocrystals were then successfully employed as a stabilizing and reducing agent in the formation of CNC/Ag nanocomposites. The structure of the cellulose was maintained throughout the reactions, which implies that Ag and Au nanoparticles were able to form and stabilize on the surface of CNCs with success. Morphological analyses further suggested and showed the formation of nanoparticles with relatively narrow size distributions.

6.2. Recommendations for Future Work

The CNC/Ag nanocomposites synthesized in this work have the potential to be used as an antimicrobial agent in the food packaging industry, whereas the CNC/Au nanocomposites can be used in catalysis. The potential applicability of these materials is, however, only deduced from the findings obtained through the various analytical techniques used. This work can therefore be extended to the actual applications of the nanocomposites. That is, a food packaging system could be designed from the CNC/Ag nanocomposites and tested against various food-borne pathogens, and the CNC/Au nanocomposites could be used to catalyze a certain reaction. In the interest of generation of new knowledge and expansion of bio-

applications, it would be interesting to study the biodegradation and thermal degradation kinetics of the nanocomposites.

6.3. Research outputs

1. Chapter in the book "Waste-to-Profit" (W-t-P): Value added Products to Generate Wealth for a Sustainable Economy, Volume 1, **Chapter 14: "Sugarcane Bagasse Waste Management":**

   https://www.novapublishers.com/catalog/product_info.php?products_id=64049

2. Research article: **Comparison of Cellulose Extraction from Sugarcane Bagasse through Alkali Treatments**, Materials Research (In press).